



TECH BRIEFS

NATIONAL AERONAUTICS AND SPACE ADMINISTRATION

-  **Technology Focus**
-  **Electronics/Computers**
-  **Software**
-  **Materials**
-  **Mechanics/Machinery**
-  **Manufacturing**
-  **Bio-Medical**
-  **Physical Sciences**
-  **Information Sciences**
-  **Books and Reports**

INTRODUCTION

Tech Briefs are short announcements of innovations originating from research and development activities of the National Aeronautics and Space Administration. They emphasize information considered likely to be transferable across industrial, regional, or disciplinary lines and are issued to encourage commercial application.

Availability of NASA Tech Briefs and TSPs

Requests for individual Tech Briefs or for Technical Support Packages (TSPs) announced herein should be addressed to

National Technology Transfer Center

Telephone No. (800) 678-6882 or via World Wide Web at www.nttc.edu

Please reference the control numbers appearing at the end of each Tech Brief. Information on NASA's Innovative Partnerships Program (IPP), its documents, and services is also available at the same facility or on the World Wide Web at <http://www.nasa.gov/offices/ipp/network/index.html>

Innovative Partnerships Offices are located at NASA field centers to provide technology-transfer access to industrial users. Inquiries can be made by contacting NASA field centers listed below.

NASA Field Centers and Program Offices

Ames Research Center

Lisa L. Lockyer
(650) 604-1754
lisa.l.lockyer@nasa.gov

Dryden Flight Research Center

Yvonne D. Gibbs
(661) 276-3720
yvonne.d.gibbs@nasa.gov

Glenn Research Center

Kathy Needham
(216) 433-2802
kathleen.k.needham@nasa.gov

Goddard Space Flight Center

Nona Cheeks
(301) 286-5810
nona.k.cheeks@nasa.gov

Jet Propulsion Laboratory

Andrew Gray
(818) 354-3821
gray@jpl.nasa.gov

Johnson Space Center

information
(281) 483-3809
jsc.techtran@mail.nasa.gov

Kennedy Space Center

David R. Makufka
(321) 867-6227
david.r.makufka@nasa.gov

Langley Research Center

Elizabeth B. Plentovich
(757) 864-2857
elizabeth.b.plentovich@nasa.gov

Marshall Space Flight Center

Jim Dowdy
(256) 544-7604
jim.dowdy@msfc.nasa.gov

Stennis Space Center

Ramona Travis
(228) 688-3832
ramona.e.travis@nasa.gov

Carl Ray, Program Executive

Small Business Innovation
Research (SBIR) & Small
Business Technology
Transfer (STTR) Programs
(202) 358-4652
carl.g.ray@nasa.gov

Doug Comstock, Director

Innovative Partnerships
Program Office
(202) 358-2221
doug.comstock@nasa.gov



TECH BRIEFS

NATIONAL AERONAUTICS AND SPACE ADMINISTRATION



5 Technology Focus: Sensors

- 5 Wirelessly Interrogated Wear or Temperature Sensors
- 6 Processing Nanostructured Sensors Using Microfabrication Techniques
- 6 Optical Pointing Sensor
- 7 Radio-Frequency Tank Eigenmode Sensor for Propellant Quantity Gauging
- 8 High-Temperature Optical Sensor



9 Electronics/Computers

- 9 Integral Battery Power Limiting Circuit for Intrinsically Safe Applications
- 9 Configurable Multi-Purpose Processor
- 10 Squeezing Alters Frequency Tuning of WGM Optical Resonator



13 Software

- 13 Automated Computer Access Request System
- 13 Range Safety for an Autonomous Flight Safety System
- 13 Fast and Easy Searching of Files in Unisys 2200 Computers
- 14 Parachute Drag Model
- 14 Evolutionary Scheduler for the Deep Space Network



15 Manufacturing & Prototyping

- 15 Modular Habitats Comprising Rigid and Inflatable Modules
- 15 More About N₂O-Based Propulsion and Breathable-Gas Systems



17 Mechanics/Machinery

- 17 Ultrasonic/Sonic Rotary-Hammer Drills
- 18 Miniature Piezoelectric Shaker for Distribution of Unconsolidated Samples to Instrument Cells
- 18 Lunar Soil Particle Separator
- 19 Advanced Aerobots for Scientific Exploration



21 Bio-Medical

- 21 Miniature Bioreactor System for Long-Term Cell Culture
- 22 Electrochemical Detection of Multiple Bioprocess Analytes
- 22 Fabrication and Modification of Nanoporous Silicon Particles
- 23 High-Altitude Hydration System



25 Physical Sciences

- 25 Photon Counting Using Edge-Detection Algorithm
- 25 Holographic Vortex Coronagraph
- 26 Optical Structural Health Monitoring Device
- 27 Fuel-Cell Power Source Based on Onboard Rocket Propellants
- 27 Polar Lunar Regions: Exploiting Natural and Augmented Thermal Environments
- 29 Simultaneous Spectral Temporal Adaptive Raman Spectrometer — SSTARs
- 29 Improved Speed and Functionality of a 580-GHz Imaging Radar
- 30 Bolometric Device Based on Fluxoid Quantization



33 Information Sciences

- 33 Algorithms for Learning Preferences for Sets of Objects
- 33 Model for Simulating a Spiral Software-Development Process
- 34 Algorithm That Synthesizes Other Algorithms for Hashing
- 34 Algorithms for High-Speed Noninvasive Eye-Tracking System
- 35 Adapting ASPEN for Orbital Express

This document was prepared under the sponsorship of the National Aeronautics and Space Administration. Neither the United States Government nor any person acting on behalf of the United States Government assumes any liability resulting from the use of the information contained in this document, or warrants that such use will be free from privately owned rights.



Wirelessly Interrogated Wear or Temperature Sensors

Such sensors could be embedded in brake pads.

Langley Research Center, Hampton, Virginia

Sensors for monitoring surface wear and/or temperature without need for wire connections have been developed. Excitation and interrogation of these sensors are accomplished by means of a magnetic-field-response recorder — an apparatus previously reported in “Magnetic-Field-Response Measurement-Acquisition System” (LAR-16908), *NASA Tech Briefs*, Vol. 30, No. 6 (June 2006), page 28. To recapitulate: The magnetic-field-response recorder is placed near,

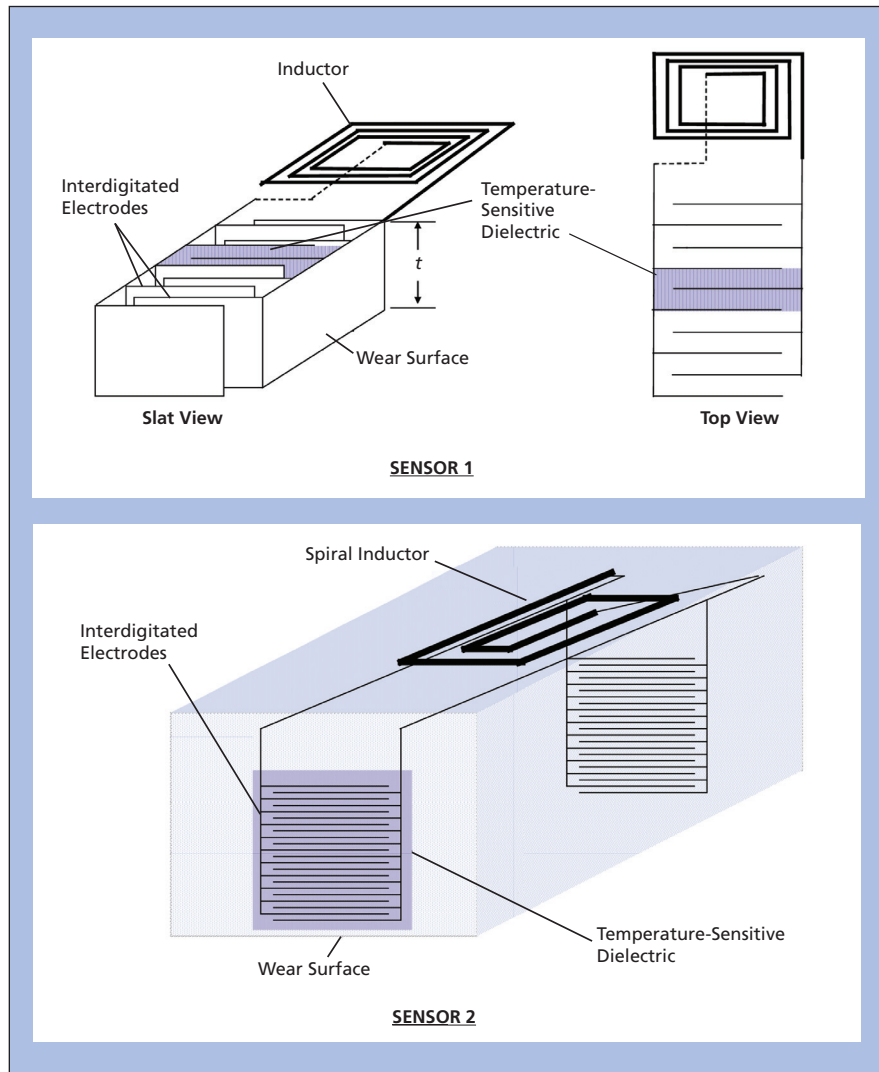
but not touching, the sensor of interest. This apparatus generates an alternating magnetic field that excites oscillations in the resonant circuit, measures the magnetic response of the circuit, and determines the resonance frequency from the response.

These sensors are related to the ones reported in “Wirelessly Interrogated Position or Displacement Sensors” (LAR-16617-1), *NASA Tech Briefs*, Vol. 31, No. 10 (October 2007), page 20. Like the

previously reported sensors, these sensors consist mainly of variable capacitors electrically connected in series with fixed inductors. In a sensor of the present type as in the previously reported ones, the capacitance and, thus, the resonance frequency, varies as a known function of the quantity of interest that one seeks to determine. Hence, the resonance frequency is measured and used to calculate the quantity of interest.

The upper part of the figure depicts one of the present sensors, wherein the capacitor consists of multiple interdigitated plate electrodes oriented perpendicular to the wear surface of, and embedded within, a block of material, the wear of which one seeks to monitor. (For example, such a sensor could be embedded in a brake pad.) The embedment is performed during the fabrication of the brake pad or other block of wearing material. The electrodes are made of a metal that becomes worn away more easily than does the material that one seeks to monitor. As the surface wears away, portions of the electrodes are also worn away, reducing the capacitance. The depth of wear can be estimated straightforwardly from the increase in the resonance frequency, using the known relationship between the change in resonance frequency and the reduction in capacitance as a function of the depth of wear.

This wear sensor can be augmented with a temperature-measurement capability by embedding, between two or more of the electrodes, a dielectric material that is temperature-sensitive in the sense that its permittivity exhibits a known variation with temperature. In this case, the capacitance, and thus the resonance frequency, depends on both the depth of wear and the temperature. Hence, if the temperature is known from a measurement by a different sensor, then the depth of wear can be determined from the resonance frequency. Similarly, if the depth of wear has been determined from a prior measurement by a different sensor (or by this sensor at a known temperature)



Capacitors Comprising Interdigitated Electrodes are connected to inductors to form resonant circuits. In both cases, the capacitance varies with the remaining thickness (t) and, thus, the depth of wear. Optionally, a temperature-sensitive dielectric can be included to obtain a temperature-measurement capability.

and there has been no wear since the prior measurement, then the present temperature can be determined from the present resonance frequency.

The lower part of the figure depicts another sensor of the present type, containing multiple sets of interdigitated elec-

trodes embedded parallel to the wearing surface in a configuration such that the number of electrode pairs, and thus the capacitance, decreases with the depth of wear. Optionally, one or more of the sets of interdigitated electrodes can be embedded along with a temperature-sensi-

tive dielectric material to obtain a temperature-measurement capability.

This work was done by Stanley E. Woodard of Langley Research Center and Bryant D. Taylor of Swales Aerospace. Further information is contained in a TSP (see page 1). LAR-16591-1

Processing Nanostructured Sensors Using Microfabrication Techniques

Nanostructured sensors have uses in safety, environmental monitoring, fire detection, and security.

John H. Glenn Research Center, Cleveland, Ohio

Standard microfabrication techniques can be implemented and scaled to help assemble nanoscale microsensors. Currently nanostructures are often deposited onto materials primarily by adding them to a solution, then applying the solution in a thin film. This results in random placement of the nanostructures with no controlled order, and no way to accurately reproduce the placement. This method changes the means by which microsensors with nanostructures are fabricated. The fundamental advantage to this approach is that it enables standard microfabrication techniques to be applied in the repeated manufacture of nanostructured sensors on a microplatform.

The fundamental steps are first to define a standard metal electrode pattern of interdigitated fingers with parallel fingers that are saw-toothed. Nanostructures are then added to a standard photoresist to form a dilute solution. The photoresist solution is then applied to

the microstructure. Before the solution solidifies, alternating electric fields are applied across the electrodes in order to align the nanostructures on the wafer. Once this photoresist later dries into a film and is processed, a second layer of metal is deposited on top of the first layer. The effect is to remove photoresist from the metal fingers, but leave the nanostructures that bridge the fingers to be held in place by the top metal layer. Longer nanostructures, which are already aligned across the fingers, will be held in place by the top metal.

This buries the contacts of the nanostructures that are bridging the fingers between two layers of metal. The result is a microsensor fabricated using microfabrication techniques with aligned nanostructures bridging the electrodes and buried electrical contacts.

Possible applications include emissions monitoring, leak detection, engine monitoring, security, fire detection, extra-vehicular-activity (EVA)

applications, personal health monitoring, and environmental monitoring. Because this process is compatible with low temperatures and thin-film supports, it can be used in thin films for conductive coatings requiring electrical connections.

A proof-of-concept of this approach was demonstrated using alumina as the substrate, metals such as platinum as the bottom electrode and titanium as the top metal layer, and both multiwalled carbon nanotubes and metal oxide nanowires as the nanostructured material.

This work was done by Gary W. Hunter, Randall L. VanderWal, Laura J. Evans, and Jennifer C. Xu of Glenn Research Center. Further information is contained in a TSP (see page 1).

Inquiries concerning rights for the commercial use of this invention should be addressed to NASA Glenn Research Center, Innovative Partnerships Office, Attn: Steve Fedor, Mail Stop 4-8, 21000 Brookpark Road, Cleveland, Ohio 44135. Refer to LEW-18418-1.

Optical Pointing Sensor

The sensor can be used as a digitizer of physical objects to extract shape data.

NASA's Jet Propulsion Laboratory, Pasadena, California

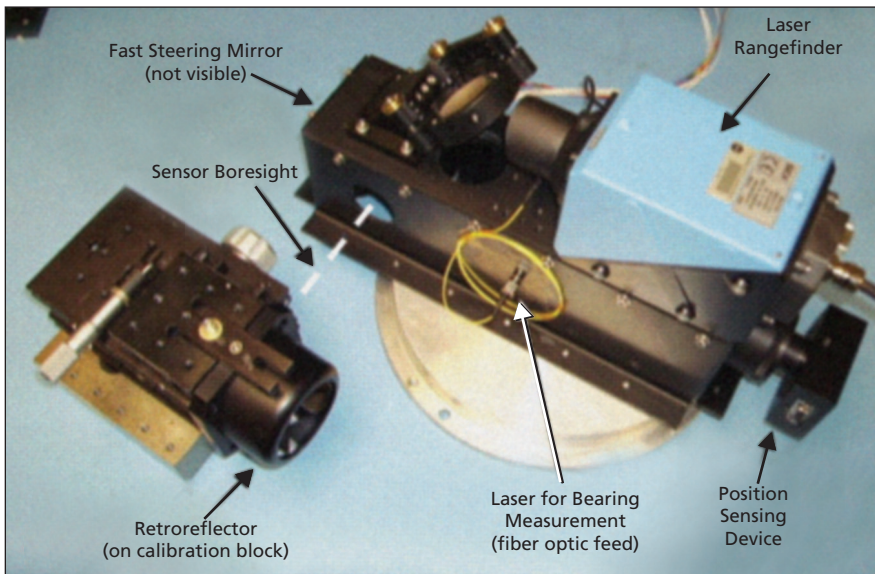
The optical pointing sensor provides a means of directly measuring the relative positions of JPL's Formation Control Testbed (FCT) vehicles without communication. This innovation is a steerable infrared (IR) rangefinder that gives measurements in terms of range and bearing to a passive retroreflector. Due to its reduced range of motion, the range and bearing measurements are on the order of 10 times

better than those of the existing sensor system.

The retroreflector is placed on one robot, and the rangefinder and steering optics are on another robot. The measurements are available on the rangefinder-mounted robot, giving it relative position knowledge to the retroreflector.

The system is composed of an HeNe pointing laser, a SICK IR laser

rangefinder, a two-axis fast steering mirror, a shear sensor, and a far-field retroreflector (see figure). The pointing laser is injected into the optical path using a beam splitter and bounces off the steering mirror toward the retroreflector. If the retroreflector is hit by the pointing laser, the beam is returned with the exact opposite direction. When the beam impact with the retroreflector is non-central,



The **Formation Control Testbed Optical Pointing Loop** hardware is shown. The sensor system is composed of a laser rangefinder, fast steering mirror, back-end shear sensor, and a large-aperture, open-face retro target.

the return will be separated (sheared) from the outgoing beam by twice the distance between the impact point and the center of the retroreflector. Provided that shear amount is small enough, the return will hit the aperture of the steering mirror and go back through the beam splitter and be

imaged on the back end of the scanner with the shear sensor. A telescope placed in front of the shear sensor serves to compress the image of the return beam to the size of the detector.

To acquire the retroreflector within the field of view of the shear sensor, the system operates by first performing an

open loop search for the retroreflector target. Once a return from the retroreflector optic is detected, a servo loop is closed with the fast steering mirror and shear sensor to center the laser beam on the vertex of the retroreflector. Once locked, any motion of the retroreflector will be tracked by keeping the servo error small. Once in track mode, the IR rangefinder can be used to give range measurements. Bearing measurements are available from a local sensor used by the steering mirror.

In comparison to flash LIDAR systems, this work represents a system with much less complexity and a lower cost. The rangefinder used by the sensor system is a low-cost COTS (commercial off-the-shelf) unit. The camera in a flash LIDAR system is replaced with a much lower cost, two-dimensional shear sensor that reports only the center of light of the image. This sensor serves as both a detector for determining whether or not the retroreflector is hit by the pointing laser and as a feedback sensor for the tracking system when the retroreflector is moving.

This work was done by Joel F. Shields and Brandon C. Metz of Caltech for NASA's Jet Propulsion Laboratory. For more information, contact iaoffice@jpl.nasa.gov. NPO-47001

Radio-Frequency Tank Eigenmode Sensor for Propellant Quantity Gauging

This sensor has applications in cryogenic liquid storage tanks.

John H. Glenn Research Center, Cleveland, Ohio

Although there are several methods for determining liquid level in a tank, there are no proven methods to quickly gauge the amount of propellant in a tank while it is in low gravity or under low-settling thrust conditions where propellant sloshing is an issue. Having the ability to quickly and accurately gauge propellant tanks in low-gravity is an enabling technology that would allow a spacecraft crew or mission control to always know the amount of propellant onboard, thus increasing the chances for a successful mission.

The Radio Frequency Mass Gauge (RFMG) technique measures the electromagnetic eigenmodes, or natural resonant frequencies, of a tank containing a dielectric fluid. The essential hardware components consist of an RF network analyzer that measures the re-

flected power from an antenna probe mounted internal to the tank. At a resonant frequency, there is a drop in the reflected power, and these inverted peaks in the reflected power spectrum are identified as the tank eigenmode frequencies using a peak-detection software algorithm. This information is passed to a pattern-matching algorithm, which compares the measured eigenmode frequencies with a database of simulated eigenmode frequencies at various fill levels. A best match between the simulated and measured frequency values occurs at some fill level, which is then reported as the gauged fill level.

The database of simulated eigenmode frequencies is created by using RF simulation software to calculate the tank eigenmodes at various fill levels. The

input to the simulations consists of a fairly high-fidelity tank model with proper dimensions and including internal tank hardware, the dielectric properties of the fluid, and a defined liquid/vapor interface. Because of small discrepancies between the model and actual hardware, the measured empty tank spectra and simulations are used to create a set of correction factors for each mode (typically in the range of 0.999–1.001), which effectively accounts for the small discrepancies. These correction factors are multiplied to the modes at all fill levels. By comparing several measured modes with the simulations, it is possible to accurately gauge the amount of propellant in the tank.

An advantage of the RFMG approach of applying computer simulations and a pattern-matching algorithm is that the

predictions can be verified through testing on Earth, and the results can be extrapolated to low-gravity liquid configurations using simulations of liquid configurations that would be likely to occur in low gravity. Such liquid configurations can also be solved using other computer software tools such as the Surface Evolver code. RF computer simulations are routinely used in the RF and communications industry to design or predict performance of RF devices. The

same software tools can be used to calculate the electromagnetic eigenmodes of large tanks with a two-phase fluid distribution. By having a pre-built library of tank eigenmode simulations, the measured tank eigenmode spectra can be compared with the library of spectra to determine the unknown amount of propellant in the tank.

This work was led by Gregory A. Zimmerli, David A. Buchanan, Jeffrey C. Follo, Karl R. Vaden, and James D. Wagner of Glenn Re-

search Center; Marius Asipauskas of National Center for Space Exploration Research; and Michael D. Herlacher of Analex Corp. Further information is contained in a TSP (see page 1).

Inquiries concerning rights for the commercial use of this invention should be addressed to NASA Glenn Research Center, Innovative Partnerships Office, Attn: Steve Fedor, Mail Stop 4-8, 21000 Brookpark Road, Cleveland, Ohio 44135. Refer to LEW-18373-1.

High-Temperature Optical Sensor

The technology significantly extends applicability of optical sensors to high-temperature environments.

John H. Glenn Research Center, Cleveland, Ohio

A high-temperature optical sensor (see Figure 1) has been developed that can operate at temperatures up to 1,000 °C. The sensor development process consists of two parts: packaging of a fiber Bragg grating into a housing that allows a more sturdy thermally stable device, and a technological process to which the device is subjected to in order to meet environmental requirements of several hundred °C.

This technology uses a newly discovered phenomenon of the formation of thermally stable secondary Bragg gratings in communication-grade fibers at high temperatures to construct robust, optical, high-temperature sensors. Testing and performance evaluation (see Figure 2) of packaged sensors demonstrated operability of the devices at 1,000 °C for several hundred hours, and during numerous thermal cycling from 400 to 800 °C with different heating rates.

The technology significantly extends applicability of optical sensors to high-temperature environments including ground testing of engines, flight propulsion control, thermal protection monitoring of launch vehicles, etc. It may also find applications in such non-aerospace arenas as monitoring of nuclear reactors, furnaces, chemical processes, and other high-temperature environments where other measurement techniques are either unreliable, dangerous, undesirable, or unavailable.

This work was done by Grigory Adamovsky, Jeffrey R. Juergens, and Donald J. Varga of

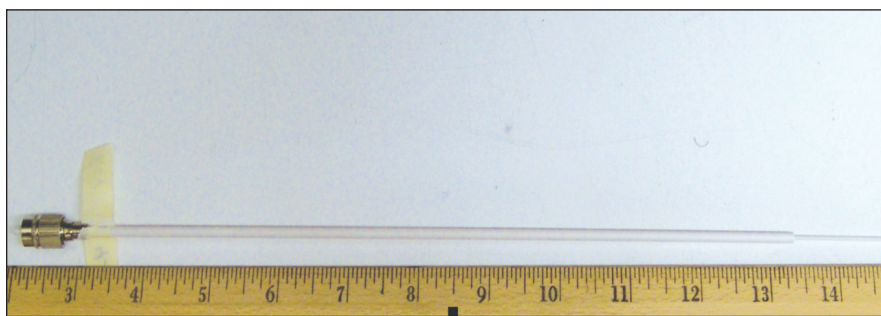


Figure 1. A Probe packaged and connectorized with a fiber Bragg grating (FBG) inside. The FBG is located at the end of the probe inside a smaller-diameter ceramic tube.

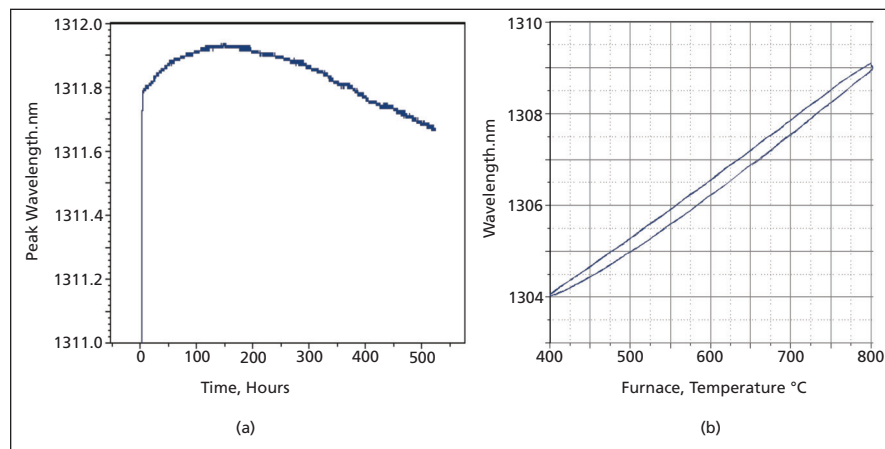


Figure 2. **Performance Characteristics:** (a) Wavelength stability of a sensor exposed to 1,000 °C for 500 hours and (b) wavelength readings as a function of temperature during thermal cycling from 400 to 800 °C.

Glenn Research Center and Bertram M. Floyd of Sierra Lobo, Inc. Further information is contained in a TSP (see page 1).

Inquiries concerning rights for the commercial use of this invention should be ad-

ressed to NASA Glenn Research Center, Innovative Partnerships Office, Attn: Steve Fedor, Mail Stop 4-8, 21000 Brookpark Road, Cleveland, Ohio 44135. Refer to LEW-18381-1.



Integral Battery Power Limiting Circuit for Intrinsically Safe Applications

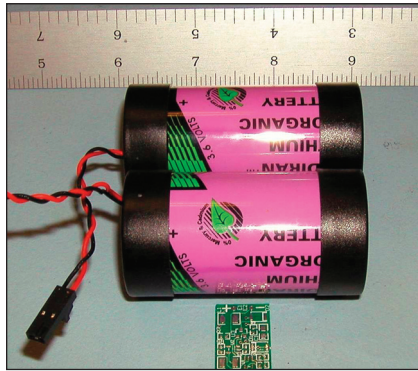
This circuit is designed for low-voltage batteries, but is valid for any DC power source.

John F. Kennedy Space Center, Florida

A circuit topology has been designed to guarantee the output of intrinsically safe power for the operation of electrical devices in a hazardous environment. This design uses a MOSFET (metal-oxide-semiconductor field-effect transistor) as a switch to connect and disconnect power to a load. A test current is provided through a separate path to the load for monitoring by a comparator against a preset threshold level. The circuit is configured so that the test current will detect a fault in the load and open the switch before the main current can respond. The main current passes through the switch and then an inductor. When a fault occurs in the load, the current through the inductor cannot change immediately, but the voltage drops immediately to safe levels.

The comparator detects this drop and opens the switch before the current in the inductor has a chance to respond. This circuit protects both the current and voltage from exceeding safe levels. Typically, this type of protection is accomplished by a fuse or a circuit breaker, but in order for a fuse or a circuit breaker to blow or trip, the current must exceed the safe levels momentarily, which may be just enough time to ignite anything in a hazardous environment. To prevent this from happening, a fuse

is typically current-limited by the addition of the resistor to keep the current within safe levels while the fuse reacts. The use of a resistor is acceptable for non-battery applications where the wasted energy and voltage drop across the resistor can be tolerated.



The **Battery Power Limiting Circuit** minimizes the voltage drop to the load, and current drain on the battery.

The use of the switch and inductor minimizes the wasted energy. For example, a circuit runs from a 3.6-V battery that must be current-limited to 200 mA. If the circuit normally draws 10 mA, then an 18-ohm resistor would drop 180 mV during normal operation, while a typical switch (0.02 ohm) and inductor (0.97 ohm) would only drop 9.9 mV. From a

power standpoint, the current-limiting resistor protection circuit wastes about 18 times more power than the switch and the inductor configuration. In the fault condition, both the resistor and the inductor react immediately. The resistor reacts by allowing more current to flow and dropping the voltage. Initially, the inductor reacts by dropping the voltage, and then by not allowing the current to change. When the comparator detects the drop in voltage, it opens the switch, thus preventing any further current flow. The inductor alone is not sufficient protection, because after the voltage drop has settled, the inductor would then allow the current to change, in this example, the current would be 3.7 A.

In the fault condition, the resistor is flowing 200 mA until the fuse blows (anywhere from 1 ms to 100 s), while the switch and inductor combination is flowing about 2 μ A test current while monitoring for the fault to be corrected. Finally, as an additional safety feature, the circuit can be configured to hold the switch opened until both the load and source are disconnected.

This work was done by Bradley M. Burns of ASRC, Inc. and Norman N. Blalock of Sierra Lobo, Inc. for Kennedy Space Center. Further information is contained in a TSP (see page 1). KSC-12703

Configurable Multi-Purpose Processor

This small processor board can be used in applications requiring substantial processing power in a flexible platform and in high vibration environments.

John F. Kennedy Space Center, Florida

Advancements in technology have allowed the miniaturization of systems used in aerospace vehicles. This technology is driven by the need for next-generation systems that provide reliable, responsive, and cost-effective range operations while providing increased capabilities such as simultaneous mission support, increased

launch trajectories, improved launch, and landing opportunities, etc.

Leveraging the newest technologies, the command and telemetry processor (CTP) concept provides for a compact, flexible, and integrated solution for flight command and telemetry systems and range systems. The CTP is a rela-

tively small circuit board that serves as a processing platform for high dynamic, high vibration environments. The CTP can be reconfigured and reprogrammed, allowing it to be adapted for many different applications. The design is centered around a configurable field-programmable gate array (FPGA) device

that contains numerous logic cells that can be used to implement traditional integrated circuits. The FPGA contains two PowerPC processors running the Vx-Works real-time operating system and are used to execute software programs specific to each application.

The CTP was designed and developed specifically to provide telemetry functions; namely, the command processing, telemetry processing, and GPS metric tracking of a flight vehicle. However, it can be used as a general-purpose processor board to perform numerous functions implemented in either hardware or software using the FPGA's processors and/or logic cells.

Functionally, the CTP was designed for range safety applications where it would ultimately become part of a vehi-

cle's flight termination system. Consequently, the major functions of the CTP are to perform the forward link command processing, GPS metric tracking, return link telemetry data processing, error detection and correction, data encryption/decryption, and initiate flight termination action commands. Also, the CTP had to be designed to survive and operate in a launch environment.

Additionally, the CTP was designed to interface with the WFF (Wallops Flight Facility) custom-designed transceiver board which is used in the Low Cost TDRSS Transceiver (LCT2) also developed by WFF. The LCT2's transceiver board demodulates commands received from the ground via the forward link and sends them to the CTP, where they are processed. The CTP inputs and

processes data from the inertial measurement unit (IMU) and the GPS receiver board, generates status data, and then sends the data to the transceiver board where it is modulated and sent to the ground via the return link.

Overall, the CTP has combined processing with the ability to interface to a GPS receiver, an IMU, and a pulse code modulation (PCM) communication link, while providing the capability to support common interfaces including Ethernet and serial interfaces boarding a relatively small-sized, lightweight package.

This work was done by J. Emilio Valencia, Christopher Forney, Robert Morrison, and Richard Burr of Kennedy Space Center. For further information, contact the Kennedy Innovative Partnerships Program Office at (321) 861-7158. KSC-13324

Squeezing Alters Frequency Tuning of WGM Optical Resonator

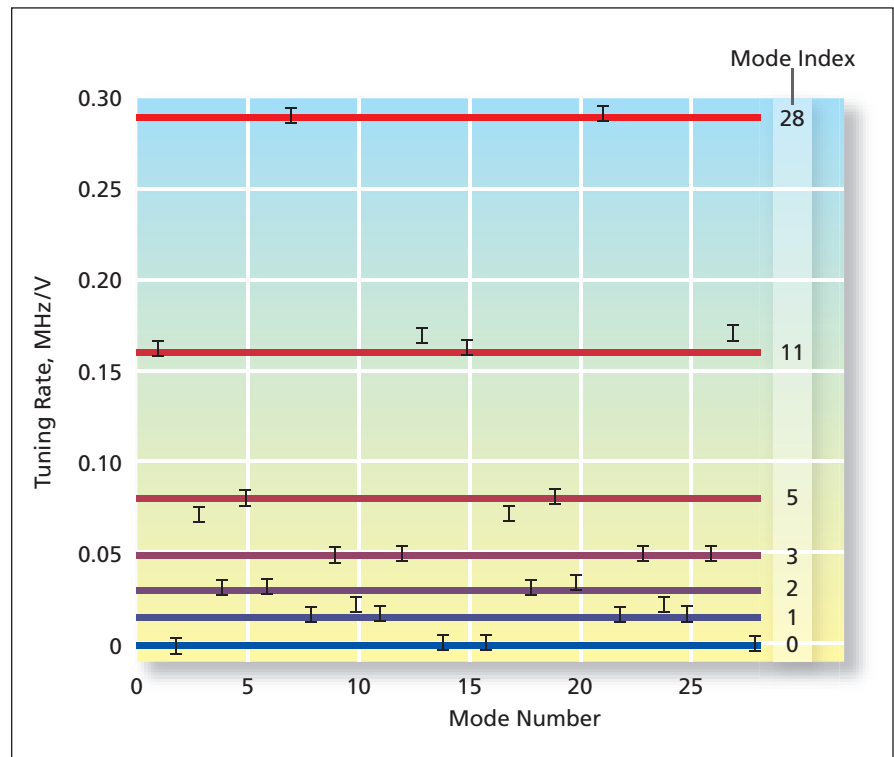
Tuning rates for modes of different indices can be made to differ.

NASA's Jet Propulsion Laboratory, Pasadena, California

Mechanical squeezing has been found to alter the frequency tuning of a whispering-gallery-mode (WGM) optical resonator that has an elliptical shape and is made of lithium niobate. It may be possible to exploit this effect to design reconfigurable optical filters for optical communications and for scientific experiments involving quantum electrodynamic.

Some background information is prerequisite to a meaningful description of the squeezing-induced alteration of frequency tuning: The spectrum of a WGM resonator is represented by a comblike plot of intensity versus frequency. Each peak of the comblike plot corresponds to an electromagnetic mode represented by an integer mode number, and the modes are grouped into sets represented by integer mode indices. Because lithium niobate is an electro-optically active material, the WGM resonator can be tuned (that is, the resonance frequencies can be shifted) by applying a suitable bias potential. The frequency shift of each mode is quantified by a tuning rate defined as the ratio between the frequency shift and the applied potential. In the absence of squeezing, all modes exhibit the same tuning rate. This concludes the background information.

It has been demonstrated experimentally that when the resonator is squeezed



Tuning Rates were calculated from resonance-frequency-vs.-voltage measurements on an elliptical WGM resonator squeezed along its semimajor axis.

along part of either of its two principal axes, tuning rates differ among the groups of modes represented by different indices (see figure). The differences in tuning rates could be utilized to con-

figure the resonance spectrum to obtain a desired effect; for example, through a combination of squeezing and electrical biasing, two resonances represented by different mode indices could be set at a

specified frequency difference — something that could not be done through electrical biasing alone.

This work was done by Makan Mohageg and Lute Maleki of Caltech for NASA's Jet Propulsion Laboratory. Further information is contained in a TSP (see page 1).

In accordance with Public Law 96-517, the contractor has elected to retain title to this invention. Inquiries concerning rights for its commercial use should be addressed to:

*Innovative Technology Assets Management
JPL
Mail Stop 202-233*

*4800 Oak Grove Drive
Pasadena, CA 91109-8099
E-mail: iaoffice@jpl.nasa.gov
Refer to NPO-45044, volume and number of this NASA Tech Briefs issue, and the page number.*



Automated Computer Access Request System

The Automated Computer Access Request (AutoCAR) system is a Web-based account provisioning application that replaces the time-consuming paper-based computer-access request process at Johnson Space Center (JSC). AutoCAR combines rules-based and role-based functionality in one application to provide a centralized system that is easily and widely accessible. The system features a work-flow engine that facilitates request routing, a user registration directory containing contact information and user metadata, an access request submission and tracking process, and a system administrator account management component. This provides full, end-to-end disposition approval chain accountability from the moment a request is submitted.

By blending both rules-based and role-based functionality, AutoCAR has the flexibility to route requests based on a user's nationality, JSC affiliation status, and other export-control requirements, while ensuring a user's request is addressed by either a primary or backup approver. All user accounts that are tracked in AutoCAR are recorded and mapped to the native operating system schema on the target platform where user accounts reside. This allows for future extensibility for supporting creation, deletion, and account management directly on the target platforms by way of AutoCAR. The system's directory-based lookup and day-to-day change analysis of directory information determines personnel moves, deletions, and additions, and automatically notifies a user via e-mail to revalidate his/her account access as a result of such changes. AutoCAR is a Microsoft classic active server page (ASP) application hosted on a Microsoft Internet Information Server (IIS).

This program was written by Bryan E. Snook from Johnson Space Center. Further information is contained in a TSP (see page 1), MSC-24174-1

Range Safety for an Autonomous Flight Safety System

The Range Safety Algorithm software encapsulates the various constructs and

algorithms required to accomplish Time Space Position Information (TSPI) data management from multiple tracking sources, autonomous mission mode detection and management, and flight-termination mission rule evaluation. The software evaluates various user-configurable rule sets that govern the qualification of TSPI data sources, provides a pre-launch autonomous hold-launch function, performs the flight-monitoring-and-termination functions, and performs end-of-mission safing.

Rule types are tailored to the Range Safety problem domain and are based on existing range practices with human-in-the-loop flight-termination systems. This module provides a cleanly deployable software library for autonomously executing a number of real-time range safety decisional functions. Its key strength is its ability to emulate the substantial variety of human-in-the-loop flight safety mission rules using a comparatively small set of flight-termination rule types. These four rules are:

1. Generic Parameter Threshold Limit – This rule is used to fire a terminate condition in response to one or more threshold conditions or Boolean truth conditions. This rule may carry with it an arbitrary number of interpolative look-up tables. It can implement flight azimuth constraints, erratic flight and attitude rate limits, and vehicle performance limits.
2. Coordinate Boundary Rule – This rule is used to determine whether or not a specified point is contained within a simple closed boundary represented by a table of coordinates. The state of a variable is evaluated using a ray crossing point-in-polygon algorithm. During each update cycle, the closest distance between the specified coordinate point and coordinate boundary is computed. These can be applied to present position, instantaneous impact point coordinates, flight corridor inclusion limits, protected area exclusion enforcement limits, and upper-stage commit limits.
3. Two-Point Gate Rule – This rule is used to determine whether or not a specified point has crossed a gate formed by a line between two points, and whether or not a specified point is ahead of or behind the gate at any point in time. These gates may be sta-

tistically located, or dynamically assigned via interpolative lookup tables. The state of a variable is computed by looking for intersections between the gate and a line formed from the previous and current locations of the target point. Another variable is computed by comparing the relative location of the specified coordinate set to the gate.

4. Trajectory Adaptable Green-Time Rule – This rule is used to establish the permissible time of flight with no valid data, and to flag a destruct condition when this time has been exceeded. Algorithms are used to compute the worst-case instantaneous impact point velocity as a function of the current state, and of vehicle acceleration.

The software is configured by the user via an XML configuration file. The algorithms are implemented within a C++ container class that can be embedded in and serviced by host application. Presently, the software possesses approximately 5,500 lines of code distributed over 28 source files.

This work was done by Raymond J. Lanzi of Goddard Space Flight Center and James C. Simpson of Kennedy Space Center. Further information is contained in a TSP (see page 1), GSC-15594-1

Fast and Easy Searching of Files in Unisys 2200 Computers

A program has been written to enable (1) fast and easy searching of symbolic files for one or more strings of characters, dates, or numerical values in specific fields or columns and (2) summarizing results of searching other fields or columns. Intended for use in Unisys 2200-series computers under OS 2200, the program implements a simplified version of a UNIX AWK command implemented in Unisys macro-assembler. (AWK is an interpreted programming language, included in most versions of UNIX, for filtering and manipulating textual data.) The program is given the name of a file or an element thereof to scan, the numbers of the fields or columns that would contain the strings of characters or numerical values that are sought, and options to control the type of search and display results. The

program uses standard Unisys library routines for reading files that have standard structures and for editing and printing output. The program can run in a batch or an interactive mode.

This program was written by James S. Sarp of United Space Alliance for Johnson Space Center. For further information, contact the Johnson Commercial Technology Office at (281) 483-3809. MSC-23855-1

Parachute Drag Model

DTV-SIM is a computer program that implements a mathematical model of the flight dynamics of a missile-shaped drop test vehicle (DTV) equipped with a multistage parachute system that includes two simultaneously deployed drogue parachutes and three main parachutes deployed subsequently and simultaneously by use of pilot parachutes. DTV-SIM was written to support air-drop tests of the DTV/parachute system, which serves a simplified prototype of a proposed crew capsule/parachute landing system.

The DTV-SIM model is of a point-mass trajectory-integrator type and includes detailed submodels of the staged deployment of, inflation of, and aerodynamic drag on, the parachutes. The model simulates (1) the forces on the parachutes and

the DTV and (2) the motion of the DTV/parachute system from release until landing. Before a planned test, DTV-SIM is used to predict the flight of the DTV/parachute system in order to develop a flight envelope for the test. After the test, DTV-SIM is used to reconstruct the flight on the basis of data acquired during the test and, while so doing, to optimize parameters in the parachute-inflation simulation submodels.

This program was written by Peter Cuthbert of Johnson Space Center. For further information, contact the Johnson Commercial Technology Office at (281) 483-3809. MSC-24361-1

Evolutionary Scheduler for the Deep Space Network

A computer program assists human schedulers in satisfying, to the maximum extent possible, competing demands from multiple spacecraft missions for utilization of the transmitting/receiving Earth stations of NASA's Deep Space Network. The program embodies a concept of optimal scheduling to attain multiple objectives in the presence of multiple constraints. Optimization of schedules is performed through a selection-and-reproduction process inspired by a biological evolution process. A

genome (a representation of design parameters in a genetic algorithm) is encoded such that a subset of the scheduling constraints (e.g., the times when a given spacecraft lies within the field of view of a given antenna) are automatically satisfied. Several fitness functions are formulated to emphasize different aspects of the scheduling problem, and multi-fitness functions are optimized simultaneously by use of multi-objective optimization algorithms.

The output of the program consists of a population of Pareto-optimal schedules that demonstrate the compromises made in solving the scheduling problem and provide insight into a conflict resolution process. These schedules are used by human schedulers to choose the simplest paths to resolution of conflicts as items on schedules are changed and as new items are added to schedules.

This program was written by Alexandre Guillaume, Seungwon Lee, Yeou-Fang Wang, Hua Zheng, Savio Chau, Yu-Wen Tung, Richard J. Terrile, and Robert Hovden of Caltech for NASA's Jet Propulsion Laboratory. For more information, contact iaoffice@jpl.nasa.gov.

This software is available for commercial licensing. Please contact Daniel Broderick of the California Institute of Technology at danielb@caltech.edu. Refer to NPO-44821.



Modular Habitats Comprising Rigid and Inflatable Modules

Potential applications include hurricane-relief housing.

Lyndon B. Johnson Space Center, Houston, Texas

Modular, lightweight, fully equipped buildings comprising hybrids of rigid and inflatable structures can be assembled on Earth and then transported to and deployed on the Moon for use as habitats. Modified versions of these buildings could also prove useful on Earth as shelters that can be rapidly and easily erected in emergency situations and/or extreme environments: examples include shelters for hurricane relief and for Antarctic exploration.

A building according to the proposal (see figure) would include a rigid composite-material module containing an inner room, plus two inflatable sections that, once inflated, would contain two anterooms. After inflation, the building as thus fully deployed (109 m³) could have a volume significantly greater than

it had when it was stowed compactly (48 m³) for transport.

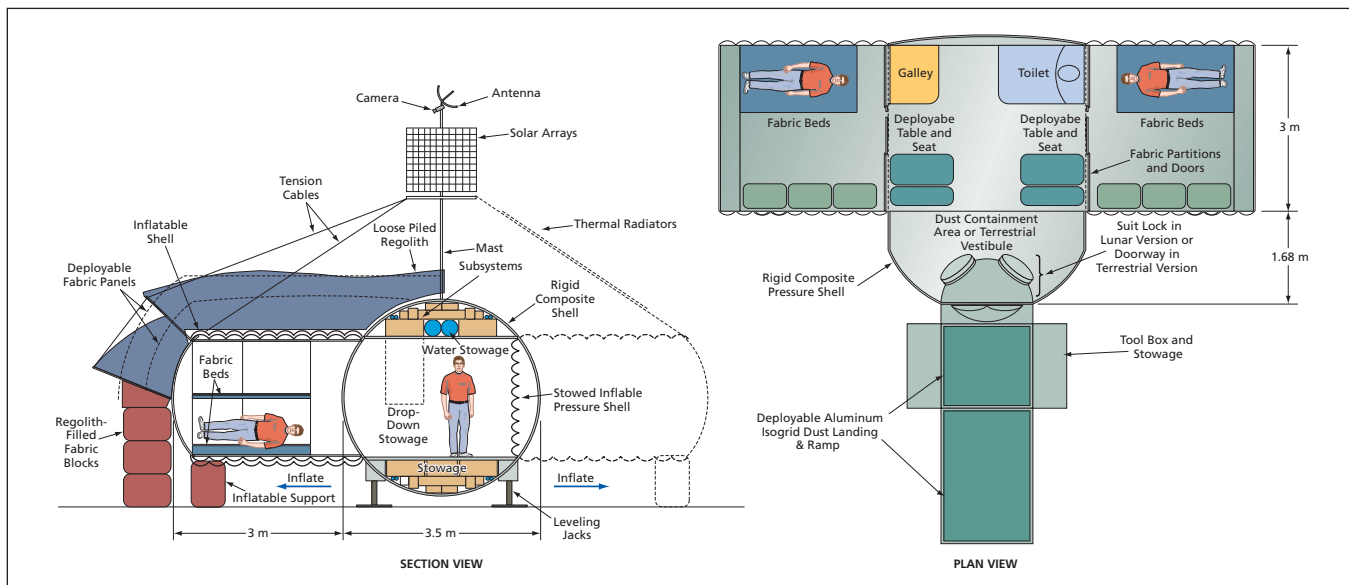
The walls of the inflatable anteroom modules would be made of a multilayer fabric-reinforced, flexible material impermeable by air, combined with high-tensile-strength cables or binding straps and with deployable rigidifying polyethylene foam. Equipment and subsystems needed for habitation would be integrated into the roof and ceiling plenum spaces of the rigid module to ensure that ducting, wiring, and plumbing all have solid connections to environmental control life support systems, avionics, power supplies, and the module structure.

Integrated into the inflatable modules would be non-flammable Nomex (or equivalent aramid) fabric floors, parti-

tions, and furniture consisting mainly of fabric beds for crewmembers. Upon inflation, the floors, partitions, beds, and any other furniture would become deployed into place.

Attached to the rigid module would be a deployable mast that would serve as both a structural element, solar array mast, and a radio-communication tower: Tension cables attached between the anterooms and the mast would support part of the weight of the anterooms. The mast could support external electronic cameras, communication antennas, and fiber-optic light collectors.

This work was done by Kriss J. Kennedy of Johnson Space Center. Further information is contained in a TSP (see page 1). MSC-24242-1



This Modular Building could be deployed rapidly for use as a habitat in a hostile environment or an emergency situation.

More About N₂O-Based Propulsion and Breathable-Gas Systems

Lyndon B. Johnson Space Center, Houston, Texas

A concept was evaluated of using nitrous oxide as (1) a monopropellant in thrusters for space suits and spacecraft and (2) a source of breathable gas inside space suits and spacecraft, both by

exploiting the controlled decomposition of N₂O into N₂ and O₂. Relative to one prior monopropellant hydrazine,

N₂O is much less toxic, yet offers comparable performance. N₂O can be

stored safely as a liquid at room temperature and unlike another prior monopropellant hydrogen peroxide does not decompose spontaneously. A prototype N₂O-based thruster has been

demonstrated. It has also been proposed to harness N₂O-based thrusters for generating electric power and to use the N₂ + O₂ decomposition product as a breathable gas. Because of the high performance, safety, and ease of handling of N₂O, it can be expected to be economically attractive to equip future spacecraft and space suits with

N₂O-based thrusters and breathable-gas systems.

This work was done by Robert Zubrin, Greg Mungas, and K. Mark Caviezel of Pioneer Astronautics for Johnson Space Center. For further information, contact the JSC Innovation Partnerships Office at (281) 483-3809.

In accordance with Public Law 96-517, the contractor has elected to retain title to

this invention. Inquiries concerning rights for its commercial use should be addressed to:

*Pioneer Astronautics
11111 West 8th Avenue, Unit-A
Lakewood, CO 80215*

Refer to MSC-23707-1, volume and number of this NASA Tech Briefs issue, and the page number.



Ultrasonic/Sonic Rotary-Hammer Drills

USDC cutting debris is removed by rotation of fluted drill bits.

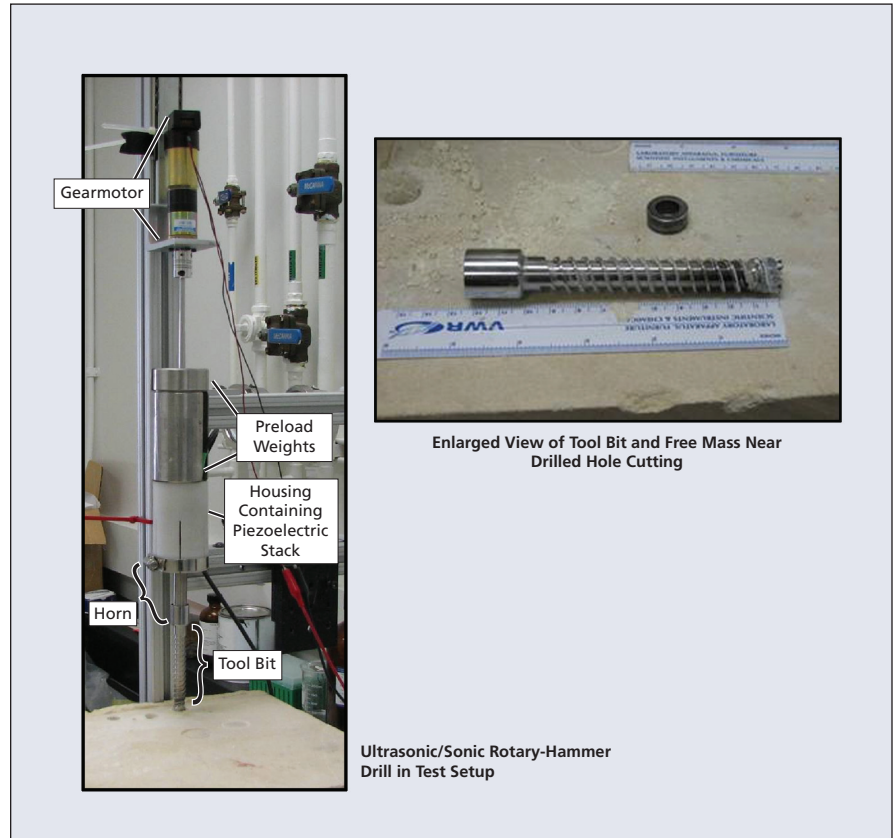
NASA's Jet Propulsion Laboratory, Pasadena, California

Ultrasonic/sonic rotary-hammer drill (USRoHD) is a recent addition to the collection of apparatuses based on ultrasonic/sonic drill corer (USDC). As described below, the USRoHD has several features, not present in a basic USDC, that increase efficiency and provide some redundancy against partial failure.

USDCs and related apparatuses were conceived for boring into, and/or acquiring samples of, rock or other hard, brittle materials of geological interest. They have been described in numerous previous *NASA Tech Briefs* articles.

To recapitulate: A USDC can be characterized as a lightweight, low-power, piezoelectrically driven jack-hammer in which ultrasonic and sonic vibrations are generated and coupled to a tool bit. A basic USDC includes a piezoelectric stack, an ultrasonic transducer horn connected to the stack, a free mass ("free" in the sense that it can bounce axially a short distance between hard stops on the horn and the bit), and a tool bit. The piezoelectric stack creates ultrasonic vibrations that are mechanically amplified by the horn. The bouncing of the free mass between the hard stops generates the hammering action (and a resulting chiseling action at the tip of the tool bit) that is more effective for drilling than is the microhammering action of ultrasonic vibrations alone. The hammering and chiseling actions are so effective that unlike in conventional twist drilling, little applied axial force is needed to make the apparatus advance into the material of interest. There are numerous potential applications for USDCs and related apparatuses in geological exploration on Earth and on remote planets.

In early USDC experiments, it was observed that accumulation of cuttings in a drilled hole causes the rate of penetration of the USDC to decrease steeply with depth, and that the rate of penetration can be increased by removing the



Ultrasonic/Sonic Rotary-Hammer Drill in Test Setup

The USRoHD Partly Resembles a Twist Drill in that it includes a USDC with a fluted tool bit, rotated by a gearmotor.

cuttings. The USRoHD concept provides for removal of cuttings in the same manner as that of a twist drill: An USRoHD includes a USDC and a motor with gearhead (see figure). The USDC provides the bit hammering and the motor provides the bit rotation. Like a twist drill bit, the shank of the tool bit of the USRoHD is fluted. As in the operation of a twist drill, the rotation of the fluted drill bit removes cuttings from the drilled hole.

The USRoHD tool bit is tipped with a replaceable crown having cutting teeth on its front surface. The teeth are shaped to promote fracturing of the rock face through a combination of hammering and rotation of the tool bit. Helical channels on the outer cylindrical surface of the crown serve as a continua-

tion of the fluted surface of the shank, helping to remove cuttings.

In the event of a failure of the USDC, the USRoHD can continue to operate with reduced efficiency as a twist drill. Similarly, in the event of a failure of the gearmotor, the USRoHD can continue to operate with reduced efficiency as a USDC.

This work was done by Mircea Badescu, Stewart Sherrit, Yoseph Bar-Cohen, Xiaoqi Bao, and Steve Kassab of Caltech for NASA's Jet Propulsion Laboratory. Further information is contained in a TSP (see page 1).

This invention is owned by NASA, and a patent application has been filed. Inquiries concerning nonexclusive or exclusive license for its commercial development should be addressed to the Patent Counsel, NASA Management Office-JPL. Refer to NPO-44765.

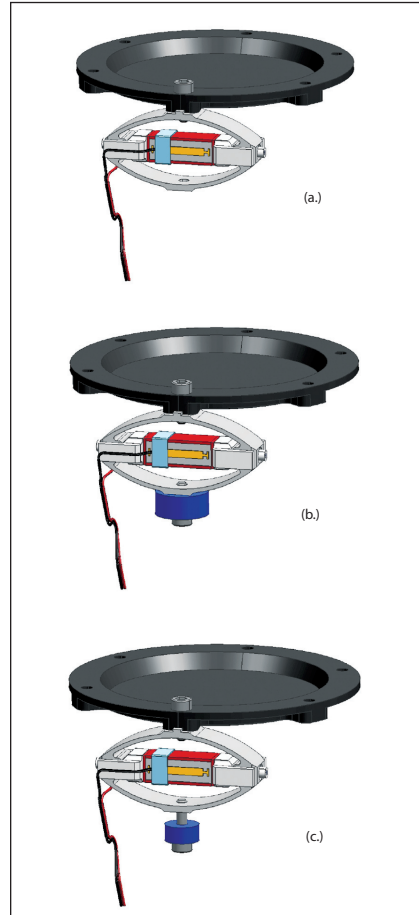
⚙️ Miniature Piezoelectric Shaker for Distribution of Unconsolidated Samples to Instrument Cells

This design could be applicable for handling powders in the pharmaceutical industry.

NASA's Jet Propulsion Laboratory, Pasadena, California

The planned Mars Science Laboratory mission requires inlet funnels for channeling unconsolidated powdered samples from the sampling and sieving mechanisms into instrument test cells, which are required to reduce cross-contamination of the samples and to minimize residue left in the funnels after each sample transport. To these ends, a solid-state shaking mechanism has been created that requires low power and is lightweight, but is sturdy enough to survive launch vibration.

The funnel mechanism is driven by asymmetrically mounted, piezoelectric flexure actuators that are out of the load path so that they do not support the funnel mass. Each actuator is a titanium, flexensional piezoelectric device driven by a piezoelectric stack. The stack has Invar endcaps with a half-spherical recess. The Invar is used to counteract the change in stress as the actuators are cooled to Mars' ambient temperatures. A ball screw is threaded through the actuator frame into the recess to apply pre-stress, and to trap the piezoelectric stack and endcaps in flexure. During the vibration cycle of the flexensional actuator frame, the compression in the piezoelectric stack may decrease to the point that it is unstressed; however, because the ball joint cannot pull, tension in the piezoelectric stack cannot be produced. The actuators are offset at 120°. In this flight design, redundancy is required, so three



A graphic of the **Actuator Mechanism** mounted on the funnel rim out of the load path. The other end of the flexure can be modified to (a) be free, (b) drive a fixed mass, or (c) drive a free mass at low resonance and produce impacts.

actuators are used though only one is needed to assist in the movement.

The funnel is supported at three contact points offset to the hexapod support contacts. The actuator surface that does not contact the ring is free to expand. Two other configurations can be used to mechanically tune the vibration. The free end can be designed to drive a fixed mass, or can be used to drive a free mass to excite impacts (see figure). Tests on this funnel mechanism show a high density of resonance modes between 1 and 20 kHz. A subset of these between 9 and 12 kHz was used to drive the CheMin actuators at 7 V peak to peak. These actuators could be driven by a single resonance, or swept through a frequency range to decrease the possibility that a portion of the funnel surface was not coincident with a nodal line (line of no displacement).

The frequency of actuation can be electrically controlled and monitored and can also be mechanically tuned by the addition of tuning mass on the free end of the actuator. The devices are solid-state and can be designed with no macroscopically moving parts. This design has been tested in a vacuum at both Mars and Earth ambient temperatures ranging from -30 to 25 °C.

This work was done by Stewart Sherrit; Curtis E Tucker, Jr.; John Frankovich, and Xiaoqi Bao of Caltech for NASA's Jet Propulsion Laboratory. Further information is contained in a TSP (see page 1). NPO-45856

⚙️ Lunar Soil Particle Separator

John H. Glenn Research Center, Cleveland, Ohio

The Lunar Soil Particle Separator (LSPS) beneficiates soil prior to *in situ* resource utilization (ISRU). It can improve ISRU oxygen yield by boosting the concentration of ilmenite, or other iron-oxide-bearing materials found in lunar soils, which can substantially reduce hydrogen reduction reactor size, as well as drastically decreasing the power input required for soil heating. LSPS particle size separations can be performed to "de-dust" regolith, and to

improve ISRU reactor flow dynamics. LSPS mineral separations can be used to alter the sintering characteristics of lunar soil, and can also be used to separate and concentrate lunar materials useful for manufacture of structural materials, glass, and chemicals.

An initial centrifugal particle size separation is integrated by the LSPS and is followed by magnetic, gravity, and/or electrostatic separations. LSPS hardware for each unit operation exhibits favor-

able properties of low mass and low power requirements. A single feeder delivers soil to the system where sorted particles cascade by gravity to the next unit operation, or to product collection bins. The centrifugal particle separator avoids the use of heavy, eccentric drives that require high power input, and does not require the use of screens that can plug with near-size particles. The magnetic separator uses high-strength, permanent magnets and requires power only to ro-

tate the separation drum. The electrostatic separator uses a high-voltage power module that generates an electrostatic field with very low power consumption. Small vibrators and smooth surfaces placed at appropriate angles are used to avoid particle hang-up.

This system is amenable to testing and operation in vacuum, and the operating parameters and hardware configurations can also be adjusted for testing and evaluation in reduced gravity.

This work was done by Mark Berggren of Pioneer Astronautics for Glenn Research Cen-

ter. Further information is contained in a TSP (see page 1).

Inquiries concerning rights for the commercial use of this invention should be addressed to NASA Glenn Research Center, Innovative Partnerships Office, Attn: Steve Fedor, Mail Stop 4-8, 21000 Brookpark Road, Cleveland, Ohio 44135. Refer to LEW-18515-1.

Advanced Aerobots for Scientific Exploration

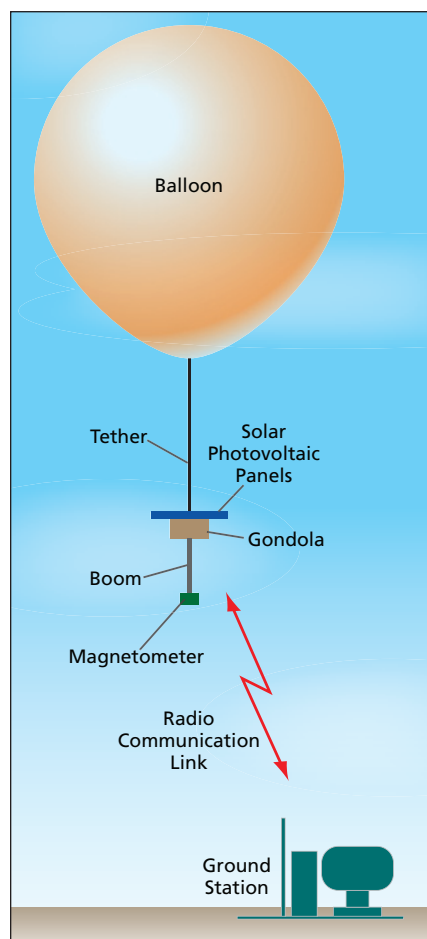
Relative to prior such aerobots, these are much less massive.

NASA's Jet Propulsion Laboratory, Pasadena, California

The Picosat and Uninhabited Aerial Vehicle Systems Engineering (PAUSE) project is developing balloon-borne instrumentation systems as aerobots for scientific exploration of remote planets and for diverse terrestrial purposes that can include scientific exploration, mapping, and military surveillance. The underlying concept of balloon-borne gondolas housing outer-space-qualified scientific instruments and associated data-processing and radio-communication equipment is not new. Instead, the novelty lies in numerous design details that, taken together, make a PAUSE aerobot smaller, less expensive, and less massive, relative to prior aerobots developed for similar purposes: Whereas the gondola (including the instrumentation system housed in it) of a typical prior aerobot has a mass of hundreds of kilograms, the mass of the gondola (with instrumentation system) of a PAUSE aerobot is a few kilograms.

The figure schematically depicts a recent PAUSE aerobot designed and built for terrestrial demonstration and testing in the development of a Mars-exploration aerobot. This aerobot includes a gondola with instrumentation system having a total mass <5 kg, the exact mass depending on which of two alternative configurations is chosen. The gondola is suspended from a 12-m-diameter helium balloon, rated at a helium gauge pressure of 5 mb (500 Pa), that is capable of supporting a load of as much as 15 kg for as long as 24 hours.

One of the instruments is a magnetometer. To isolate the magnetometer sensor head from magnetic fields generated by other equipment, the magnetometer sensor head is mounted at the outer end of 0.8-m-long fiberglass boom that extends from the gondola. Also



This Aerobot is a prototype of planetary-exploration and terrestrial aerobots having masses of only a few kilograms.

mounted on the boom are an external-temperature sensor and a downward-looking electronic camera containing a complementary metal oxide/semiconductor (CMOS) image sensor.

The gondola houses the magnetometer boards; two other CMOS imagers (one aimed upward, the other aimed

horizontally); a spread-spectrum radio transceiver operating at a nominal carrier frequency of 900 MHz; a flash electronic memory having a capacity of 1GB; a single-board computer; a pressure sensor; lithium primary batteries in one configuration or solar photovoltaic panels (on top of the gondola) and lithium-ion rechargeable batteries in the other configuration; a battery-current sensor; a serial multiplexer; voltage converters; a Global Positioning System (GPS) receiver; and an inertial measurement unit (IMU) that consists of accelerometers, gyroscopes, and magnetometers for all three coordinate axes.

The single-board computer takes temperature, pressure, IMU, battery current and voltage, and GPS readings at time intervals of one second. The magnetometer data are read at a repetition rate of 4 Hz, and an average of four successive readings is recorded every second. The cameras are set to automatically acquire images at intervals of five minutes, but they can also be commanded to acquire images at any time. The data (including digitized images) are both stored in the flash memory and transmitted via the radio transceiver to a ground station. The data transmissions are programmed to take place at set intervals; in addition, data transmissions can also be commanded at any time from the ground station. The instrumentation system has an average power demand <4 W, with occasional jumps to 7 W during transmission of data.

This work was done by Alberto Behar, Carol A. Raymond, Jaret B. Matthews, Fabien Nicaise, and Jack A. Jones of Caltech for NASA's Jet Propulsion Laboratory. Further information is contained in a TSP (see page 1). NPO-42737



Miniature Bioreactor System for Long-Term Cell Culture

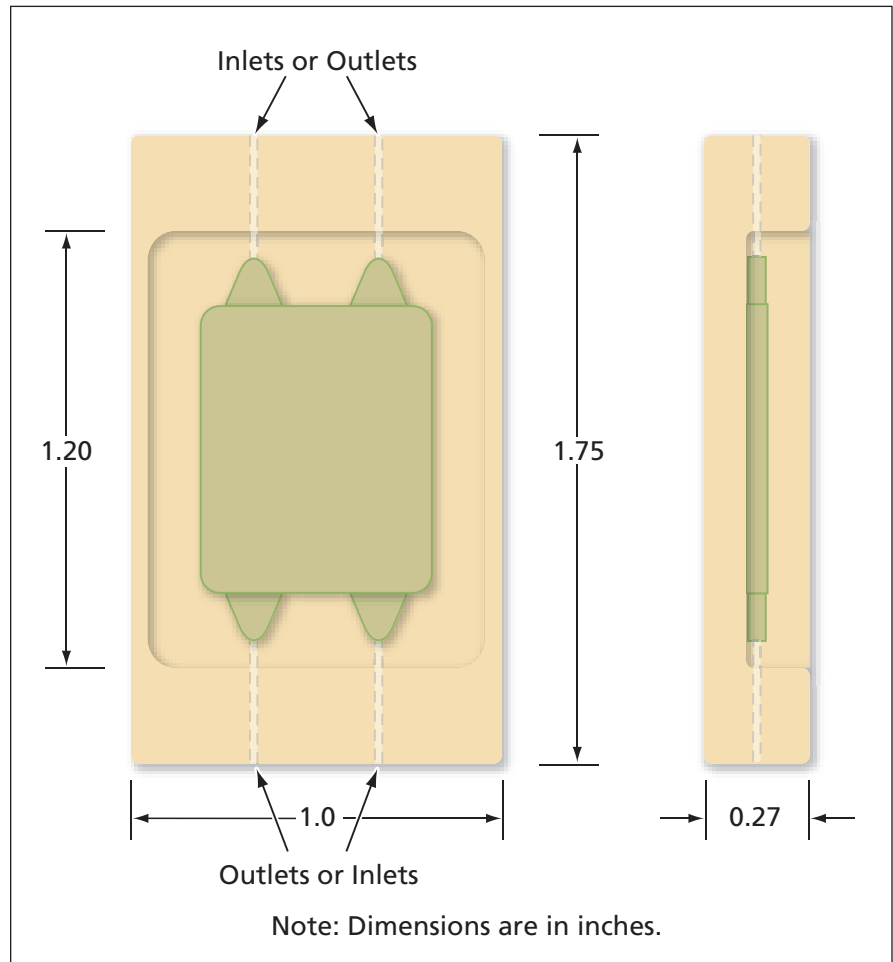
Cells can be cultured and sampled with minimal human intervention.

Lyndon B. Johnson Space Center, Houston, Texas

A prototype miniature bioreactor system is designed to serve as a laboratory benchtop cell-culturing system that minimizes the need for relatively expensive equipment and reagents and can be operated under computer control, thereby reducing the time and effort required of human investigators and reducing uncertainty in results. The system includes a bioreactor, a fluid-handling subsystem, a chamber wherein the bioreactor is maintained in a controlled atmosphere at a controlled temperature, and associated control subsystems. The system can be used to culture both anchorage-dependent and suspension cells, which can be either prokaryotic or eukaryotic. Cells can be cultured for extended periods of time in this system, and samples of cells can be extracted and analyzed at specified intervals. By integrating this system with one or more microanalytical instrument(s), one can construct a complete automated analytical system that can be tailored to perform one or more of a large variety of assays.

The bioreactor (see figure) is a thin culture chamber that has two or more inlets and two or more outlets for flows of liquids. The top face of the chamber is bounded by a membrane of porous respiratory active material that enables exchange of O₂ and CO₂ between the cell culture and the controlled atmosphere in which the bioreactor resides. The bottom face of the chamber can be either a second porous membrane or a microscope cover sheet, which enables microscopic imaging of cells in the chamber.

The fluid-handling subsystem includes an upstream and a downstream switching valve, flexible tubes that connect the upstream switching valve with three supply reservoirs and the bioreactor inlets, flexible tubes that connect the downstream switching valve with the bioreactor outlets and with waste and sampling reservoirs, and a peristaltic pump. The tubes on the downstream side are draped along the roller bearings of the peristaltic pump. There are three supply reservoirs: one containing the cell-culture nutrient medium, one con-



The **Bioreactor** is a thin culture chamber with inlets and outlets for liquids. The working volume of the bioreactor is 1 mL. Alternative designs can provide for more than the two inlets and/or for more than the two outlets shown here.

taining a phosphate buffer solution (PBS), and one containing trypsin.

The flow passages in the valves are arranged so as to allow only the one correct liquid to flow through a given tube at a given time. The upstream valve enables the selection of flow of either fresh nutrient medium or PBS to the inlets. Alternatively, for the purpose of effective disconnection of part of the bioreactor, the upstream valve can be set to infuse trypsin through one inlet and the nutrient medium through the other inlet. The downstream valve can be set to connect all outlets to the waste reservoir or

to connect a specified outlet or all outlets to a sampling reservoir.

Because the rates of flow required to sustain cell cultures are small and the system is operated accordingly, the flow velocity in the thin culture chamber is so small that the flow can be considered to be essentially laminar and two-dimensional, so that a given infinitesimal volume of liquid can be considered to travel smoothly along a simple, well-defined path. This flow characteristic can be exploited in harvesting cells from a specific region of a culture of anchorage-dependent cells, without disturbing

cells from other regions. In the case of suspension cells, harvesting is performed upon the infusion of fresh nutrient medium. Incorporated into the miniature culture system is a temperature-control system and gas-control loop. The inclusion of these two systems will enable the miniature culture system to be autonomous.

This work was done by Steve R. Gonda of Johnson Space Center and Stanley J. Kleis and Sandra K. Geffert of the University of Houston.

In accordance with Public Law 96-517, the contractor has elected to retain title to this invention. Inquiries concerning rights for its commercial use should be addressed to: Emmanuelle Schuler, Ph.D

*Technology Transfer Associate
Office of Intellectual Property Management
University of Houston
316 E. Cullen
Houston, TX 77204-2015
E-mail: eschuler@uh.edu
Refer to MSC-24210-1, volume and number of this NASA Tech Briefs issue, and the page number.*

Electrochemical Detection of Multiple Bioprocess Analytes

Key analytes can be detected using sample volumes of only 100 μ L.

Lyndon B. Johnson Space Center, Houston, Texas

An apparatus that includes highly miniaturized thin-film electrochemical sensor array has been demonstrated as a prototype of instruments for simultaneous detection of multiple substances of interest (analytes) and measurement of acidity or alkalinity in bioprocess streams. Measurements of pH and of concentrations of nutrients and wastes in cell-culture media, made by use of these instruments, are to be used as feedback for optimizing the growth of cells or the production of desired substances by the cultured cells. The apparatus is designed to utilize samples of minimal volume so as to minimize any perturbation of monitored processes.

The apparatus can function in a potentiometric mode (for measuring pH), an amperometric mode (detecting analytes via oxidation/reduction reactions), or both. The sensor array is planar and includes multiple thin-film microelectrodes covered with hydrous iridium oxide. The oxide layer on each electrode serves as both a protective and electrochemical transducing layer. In its trans-

ducing role, the oxide provides electrical conductivity for amperometric measurement or pH response for potentiometric measurement. The oxide on an electrode can also serve as a matrix for one or more enzymes that render the electrode sensitive to a specific analyte. In addition to transducing electrodes, the array includes electrodes for potential control. The array can be fabricated by techniques familiar to the microelectronics industry.

The sensor array is housed in a thin-film liquid-flow cell that has a total volume of about 100 μ L. The flow cell is connected to a computer-controlled subsystem that periodically draws samples from the bioprocess stream to be monitored. Before entering the cell, each 100- μ L sample is subjected to tangential-flow filtration to remove particles. In the present version of the apparatus, the electrodes are operated under control by a potentiostat and are used to simultaneously measure the pH and the concentration of glucose. It is anticipated that development of procedures

for trapping more enzymes into hydrous iridium oxide (and possibly into other electroactive metal oxides) and of means for imparting long-term stability to the transducer layers should make it possible to monitor concentrations of products of many enzyme reactions — for example, such key bioprocess analytes as amino acids, vitamins, lactose, and acetate.

This work was done by R. David Rauh of EIC Laboratories, Inc., for Johnson Space Center. Further information is contained in a TSP (see page 1).

In accordance with Public Law 96-517, the contractor has elected to retain title to this invention. Inquiries concerning rights for its commercial use should be addressed to:

*Jeffrey L. Bursell,
Controller/Contract Administrator
EIC Laboratories, Inc.
111 Downey Street,
Norwood, MA 02062
Phone No.: (781) 769-9450*

Refer to MSC-23578-1, volume and number of this NASA Tech Briefs issue, and the page number.

Fabrication and Modification of Nanoporous Silicon Particles

Biodegradable drug carriers allow sustained drug release for days or even weeks.

Lyndon B. Johnson Space Center, Houston, Texas

Silicon-based nanoporous particles as biodegradable drug carriers are advantageous in permeation, controlled release, and targeting. The use of biodegradable nanoporous silicon and silicon dioxide, with proper surface treatments, allows sustained drug release within the target site over a period of days, or even weeks, due to selective surface coating. A variety of surface treatment protocols are

available for silicon-based particles to be stabilized, functionalized, or modified as required. Coated polyethylene glycol (PEG) chains showed the effective depression of both plasma protein adsorption and cell attachment to the modified surfaces, as well as the advantage of long circulating.

Porous silicon particles are micromachined by lithography. Compared to the

synthesis route of the nanomaterials, the advantages include: (1) the capability to make different shapes, not only spherical particles but also square, rectangular, or ellipse cross sections, etc.; (2) the capability for very precise dimension control; (3) the capacity for porosity and pore profile control; and (4) allowance of complex surface modification. The particle patterns as small as 60 nm can

be fabricated using the state-of-the-art photolithography. The pores in silicon can be fabricated by exposing the silicon in an HF/ethanol solution and then subjecting the pores to an electrical current. The size and shape of the pores inside silicon can be adjusted by the doping of the silicon, electrical current application, the composition of the electrolyte solution, and etching time.

The surface of the silicon particles can be modified by many means to provide targeted delivery and on-site permanence for extended release. Multiple active agents can be co-loaded into the particles. Because the surface modification of particles can be done on wafers before the mechanical release, asymmetrical surface modification is feasible.

Starting from silicon wafers, a treatment, such as KOH dipping or reactive-

ion etching (RIE), may be applied to make the surface rough. This helps remove the nucleation layer. A protective layer is then deposited on the wafer. The protective layer, such as silicon nitride film or photoresist film, protects the wafer from electrochemical etching in an HF-based solution. A lithography technique is applied to pattern the particles onto the protective film. The undesired area of the protective film is removed, and the protective film on the back side of the wafer is also removed. Then the pattern is exposed to HF/surfactant solution, and a larger DC electrical current is applied to the wafers for a selected time. This step removes the nucleation layer. Then a DC current is applied to generate the nanopores. Next, a large electrical current is applied to generate a release layer. The particles are mechanically suspended in the sol-

vent and collected by filtration or centrifuge.

This work was done by Mauro Ferrari and Xuewu Liu of the University of Texas Health Science Center for Johnson Space Center. For further information, contact the Johnson Technology Transfer Office at (281) 483-3809.

In accordance with Public Law 96-517, the contractor has elected to retain title to this invention. Inquiries concerning rights for its commercial use should be addressed to:

*Office of Technology Management
The University of Texas
Health and Science Center at Houston
7000 Fannin, Suite 720
Houston, TX 77030*

E-mail: utsch-otm@uth.tmc.edu

Refer to MSC-24479-1, volume and number of this NASA Tech Briefs issue, and the page number.

High-Altitude Hydration System

Multiple methods of keeping water from freezing can be used by law enforcement personnel, skiers, and campers, and underwater by military personnel.

Lyndon B. Johnson Space Center, Houston, Texas

Three methods are being developed for keeping water from freezing during high-altitude climbs so that mountaineers can remain hydrated. Three strategies have been developed. At the time of this reporting two needed to be tested in the field and one was conceptual.

The first method is Passive Thermal Control Using Aerogels. This involves mounting the fluid reservoir of the climber's canteen to an inner layer of clothing for better heat retention. For the field test, bottles were mounted to the inner fleece layer of clothing, and then aerogel insulation was placed on the outside of the bottle, and circumferentially around the drink straw. When climbers need to drink, they can pull up the insulated straw from underneath the down suit, take a sip, and then put it back into the relative warmth of the suit.

For the field test, a data logger assessed the temperatures of the water reservoir, as well as near the tip of the drink straw.

The second method is Passive Thermal Control with Copper-Shielded Drink Straw and Aerogels, also mounted to inner layers of clothing for better heat retention. Braided wire emanates from the inside of the fleece jacket layer, and continues up and around the drink straw in order to use body heat to keep the system-critical drink straw warm enough to keep water in the liquid state. For the field test, a data logger will be used to compare this with the above concept.

The third, and still conceptual, method is Active Thermal Control with Microcontroller. If the above methods do not work, microcontrollers and tape heaters have been identified that could

keep the drink straw warm even under extremely cold conditions. Power requirements are not yet determined because the thermal environment inside the down suit relative to the external environment has not been established. A data logger will be used to track both the external and internal temperatures of the suit on a summit day.

This work was done by Scott E. Parazyński, Evelyne Orndoff, and Grant C. Bue of Johnson Space Center and Mark E. Schaeffbauer and Kase Urban of Jacobs Technology. For further information, contact the JSC Innovation Partnerships Office at (281) 483-3809.

This invention is owned by NASA, and a patent application has been filed. Inquiries concerning nonexclusive or exclusive license for its commercial development should be addressed to the Patent Counsel, Johnson Space Center, (281) 483-1003. Refer to MSC-24490-1.



Photon Counting Using Edge-Detection Algorithm

Improved optical communications links can be used in building-to-building networks in high-attenuation conditions such as rain or fog.

NASA's Jet Propulsion Laboratory, Pasadena, California

New applications such as high-data-rate, photon-starved, free-space optical communications require photon counting at flux rates into gigaphoton-per-second regimes coupled with subnanosecond timing accuracy. Current single-photon detectors that are capable of handling such operating conditions are designed in an array format and produce output pulses that span multiple sample times. In order to discern one pulse from another and not to overcount the number of incoming photons, a detection algorithm must be applied to the sampled detector output pulses. As flux rates increase, the ability to implement such a detection algorithm becomes difficult within a digital processor that may reside within a field-programmable gate array (FPGA).

Systems have been developed and implemented to both characterize gigahertz bandwidth single-photon detectors, as well as process photon count signals at rates into gigaphotons per second in order to implement communications links at SCPPM (serial concatenated pulse position modulation) encoded data rates exceeding 100 megabits per second with efficiencies greater than two bits per detected photon.

A hardware edge-detection algorithm and corresponding signal combining and deserialization hardware were developed to meet these requirements at sample rates up to 10 GHz. The photon discriminator deserializer hardware board accepts four inputs, which allows for the ability to take inputs from a quadphoton counting detector, to support requirements for optical tracking with a reduced number of hardware components. The four inputs are hardware leading-edge detected independently. After leading-edge detection, the resultant samples are "ORed" together prior to deserialization. The deserialization is performed to reduce the rate at which data is passed to a digital signal processor, perhaps residing within an FPGA.

The hardware implements four separate analog inputs that are connected through RF connectors. Each analog input is fed to a high-speed 1-bit comparator, which digitizes the input referenced to an adjustable threshold value. This results in four independent serial sample streams of binary 1s and 0s, which are ORed together at rates up to 10 GHz. This single serial stream is then deserialized by a factor of 16 to

create 16 signal lines at a rate of 622.5 MHz or lower for input to a high-speed digital processor assembly.

The new design and corresponding hardware can be employed with a quad-photon counting detector capable of handling photon rates on the order of multi-gigaphotons per second, whereas prior art was only capable of handling a single input at 1/4 the flux rate. Additionally, the hardware edge-detection algorithm has provided the ability to process 3–10× higher photon flux rates than previously possible by removing the limitation that photon-counting detector output pulses on multiple channels being ORed not overlap. Now, only the leading edges of the pulses are required to not overlap. This new photon counting digitizer hardware architecture supports a universal front end for an optical communications receiver operating at data rates from kilobits to over one gigabit per second to meet increased mission data volume requirements.

This work was done by Jonathan W. Gin, Danh H. Nguyen, and William H. Farr of Caltech for NASA's Jet Propulsion Laboratory. For more information, contact iaoffice@jpl.nasa.gov. NPO-47046

Holographic Vortex Coronagraph

This apparatus offers potential advantages of performance and manufacturability over conventional coronagraphs.

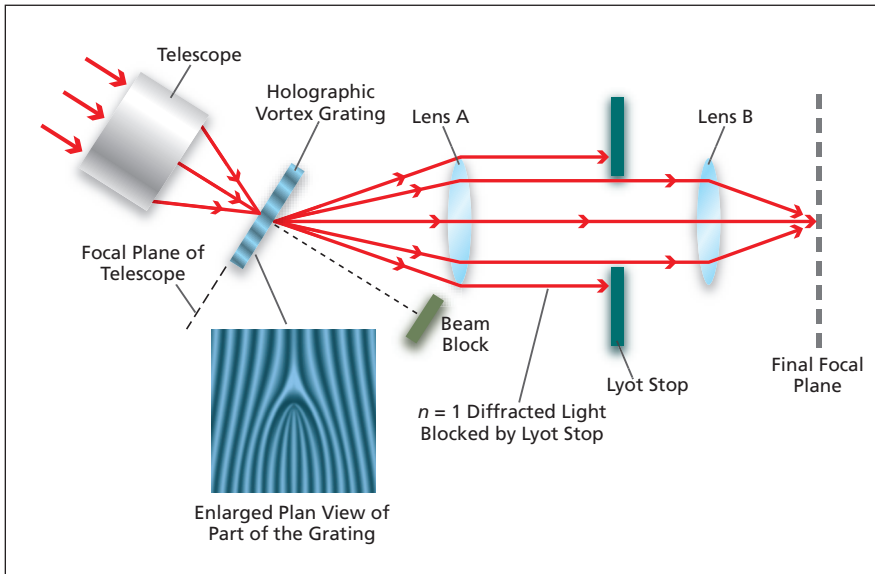
NASA's Jet Propulsion Laboratory, Pasadena, California

A holographic vortex coronagraph (HVC) has been proposed as an improvement over conventional coronagraphs for use in high-contrast astronomical imaging for detecting planets, dust disks, and other broadband light scatterers in the vicinities of stars other than the Sun. Because such light scatterers are so faint relative to their parent stars, in order to be able to detect them, it is necessary to effect ultra-high-con-

trast (typically by a factor of the order of 10^{10}) suppression of broadband light from the stars. Unfortunately, the performances of conventional coronagraphs are limited by low throughput, dispersion, and difficulty of satisfying challenging manufacturing requirements. The HVC concept offers the potential to overcome these limitations.

A key feature of any coronagraph is an occulting mask in the image plane of

a telescope, centered on the optical axis of the telescope. In a conventional coronagraph, the occulting mask is an opaque amplitude mask that obstructs the central starlight when the optical axis points toward the star in question. In the HVC, the occulting mask is a holographic vortex grating, which may be created by etching or otherwise forming the interference pattern of a helical phase ramp and a plane wave beam into



In a **Holographic Vortex Coronagraph**, a telescope would focus light onto a blazed first-order vortex grating. A beam block would absorb residual undiffracted light. Lens A would collimate the first-order-diffracted light, forming an exit pupil wherein a Lyot stop would be placed. Lens B would re-image the light transmitted through the Lyot stop to the final focal plane.

an optical surface. As shown in the figure, the interference pattern has a forked appearance.

Light incident perpendicular to the grating is diffracted into discrete orders at angles given by $\theta_n = \sin^{-1}(n\lambda/d)$, where n is the diffraction order, λ is the wavelength of the diffracted light, and d is the lateral distance between adjacent grooves in the grating. In addition, the

grating could be blazed to concentrate the diffracted light primarily into one order. If the grating is blazed to concentrate the light into the first ($n = 1$) order, then almost all of the light from a star or any other on-axis source will be transformed into a beam having a helical wavefront. Total destructive interference occurs along the axis of the helix over a broad wavelength band, attenuat-

ing the light from the star or other on-axis source.

The holographic vortex grating in the HVC is placed at the focus of the telescope and is designed and fabricated so as to almost completely suppress light from an on-axis star without significantly affecting images of planets or other light scatterers near the star. The starlight removed from the exit pupil appears outside exit pupil, whereas the light from scatterers near the star appears within the exit pupil. A Lyot stop — an aperture stop to block the starlight while passing the light from nearby scatterers — is placed in the exit pupil.

On the basis of previous research, it is anticipated that in comparison with a conventional coronagraph, the HVC would be less sensitive to aberrations, would yield higher throughput of light from scatterers near stars, and would offer greater planet/star contrast. On the basis of previous achievements in the fabrication of gratings similar to holographic vortex gratings, it appears that the grating for the HVC could readily be fabricated to satisfy initial requirements for imaging of extrasolar planets.

This work was done by David Palacios of Caltech for NASA's Jet Propulsion Laboratory. Further information is contained in a TSP (see page 1). NPO-45047

Optical Structural Health Monitoring Device

This device detects microscopic cracks and surface structural changes in components.

Dryden Flight Research Center, Edwards, California

This non-destructive, optical fatigue detection and monitoring system relies on a small and unobtrusive light-scattering sensor that is installed on a component at the beginning of its life in order to periodically scan the component *in situ*. The method involves using a laser beam to scan the surface of the monitored component. The device scans a laser spot over a metal surface to which it is attached. As the laser beam scans the surface, disruptions in the surface cause increases in scattered light intensity. As the disruptions in the surface grow, they will cause the light to scatter more. Over time, the scattering intensities over the scanned line can be compared to detect changes in the metal surface to find cracks, crack precursors, or corrosion. This periodic monitoring of the surface

can be used to indicate the degree of fatigue damage on a component and allow one to predict the remaining life and/or incipient mechanical failure of the monitored component.

This wireless, compact device can operate for long periods under its own battery power and could one day use harvested power. The prototype device uses the popular open-source TinyOS operating system on an off-the-shelf Mica2 sensor mote, which allows wireless command and control through dynamically reconfigurable multi-node sensor networks. The small size and long life of this device could make it possible for the nodes to be installed and left in place over the course of years, and with wireless communication, data can be extracted from the

nodes by operators without physical access to the devices.

While a prototype has been demonstrated at the time of this reporting, further work is required in the system's development to take this technology into the field, especially to improve its power management and ruggedness. It should be possible to reduce the size and sensitivity as well. Establishment of better prognostic methods based on these data is also needed. The increase of surface roughness with fatigue is closely connected to the microstructure of the metal, and ongoing research is seeking to connect this observed evidence of the fatigue state with microstructural theories of fatigue evolution to allow more accurate prognosis of remaining component life. Plans are also being discussed

for flight testing, perhaps on NASA's SOFIA platform.

This work was done by Benjamin D. Buckner and Vladimir Markov of MetroLaser, Inc. and James C. Earthman of the University of California for Dryden Flight Research Center.

Title to this invention, covered by U.S. Patent No. 7,221,445, has been waived under the provisions of the National Aeronautics and Space Act (42 U.S.C. 2457 (f)). Inquiries concerning licenses for its commercial development should be ad-

dressed to MetroLaser Inc. 8 Chrysler, Irvine CA 92618 Refer to DRC-007-065, volume and number of this NASA Tech Briefs issue, and the page number. Refer to DRC-007-065.

Fuel-Cell Power Source Based on Onboard Rocket Propellants

This high-energy density power source is an alternative to radioisotopes or primary batteries.

NASA's Jet Propulsion Laboratory, Pasadena, California

The use of onboard rocket propellants (dense liquids at room temperature) in place of conventional cryogenic fuel-cell reactants (hydrogen and oxygen) eliminates the mass penalties associated with cryocooling and boil-off. The high energy content and density of the rocket propellants will also require no additional chemical processing.

For a 30-day mission on the Moon that requires a continuous 100 watts of power, the reactant mass and volume would be reduced by 15 and 50 percent, respectively, even without accounting for boil-off losses. The savings increase further with increasing transit times. A high-temperature, solid oxide, electrolyte-based

fuel-cell configuration, that can rapidly combine rocket propellants — both monopropellant system with hydrazine and bi-propellant systems such as monomethyl hydrazine/ unsymmetrical dimethyl hydrazine (MMH/UDMH) and nitrogen tetroxide (NTO) to produce electrical energy — overcomes the severe drawbacks of earlier attempts in 1963–1967 of using fuel reforming and aqueous media. The electrical energy available from such a fuel cell operating at 60-percent efficiency is estimated to be 1,500 Wh/kg of reactants. The proposed use of zirconia-based oxide electrolyte at 800–1,000 °C will permit continuous operation, very high power densities, and

substantially increased efficiency of conversion over any of the earlier attempts. The solid oxide fuel cell is also tolerant to a wide range of environmental temperatures. Such a system is built for easy refueling for exploration missions and for the ability to turn on after several years of transit. Specific examples of future missions are *in-situ* landers on Europa and Titan that will face extreme radiation and temperature environments, flyby missions to Saturn, and landed missions on the Moon with 14 day/night cycles.

This work was done by Gani Ganapathi and Sri Narayan of Caltech for NASA's Jet Propulsion Laboratory. Further information is contained in a TSP (see page 1). NPO-44977

Polar Lunar Regions: Exploiting Natural and Augmented Thermal Environments

High vacuum cryogenic environments can be augmented with lightweight thermal shielding.

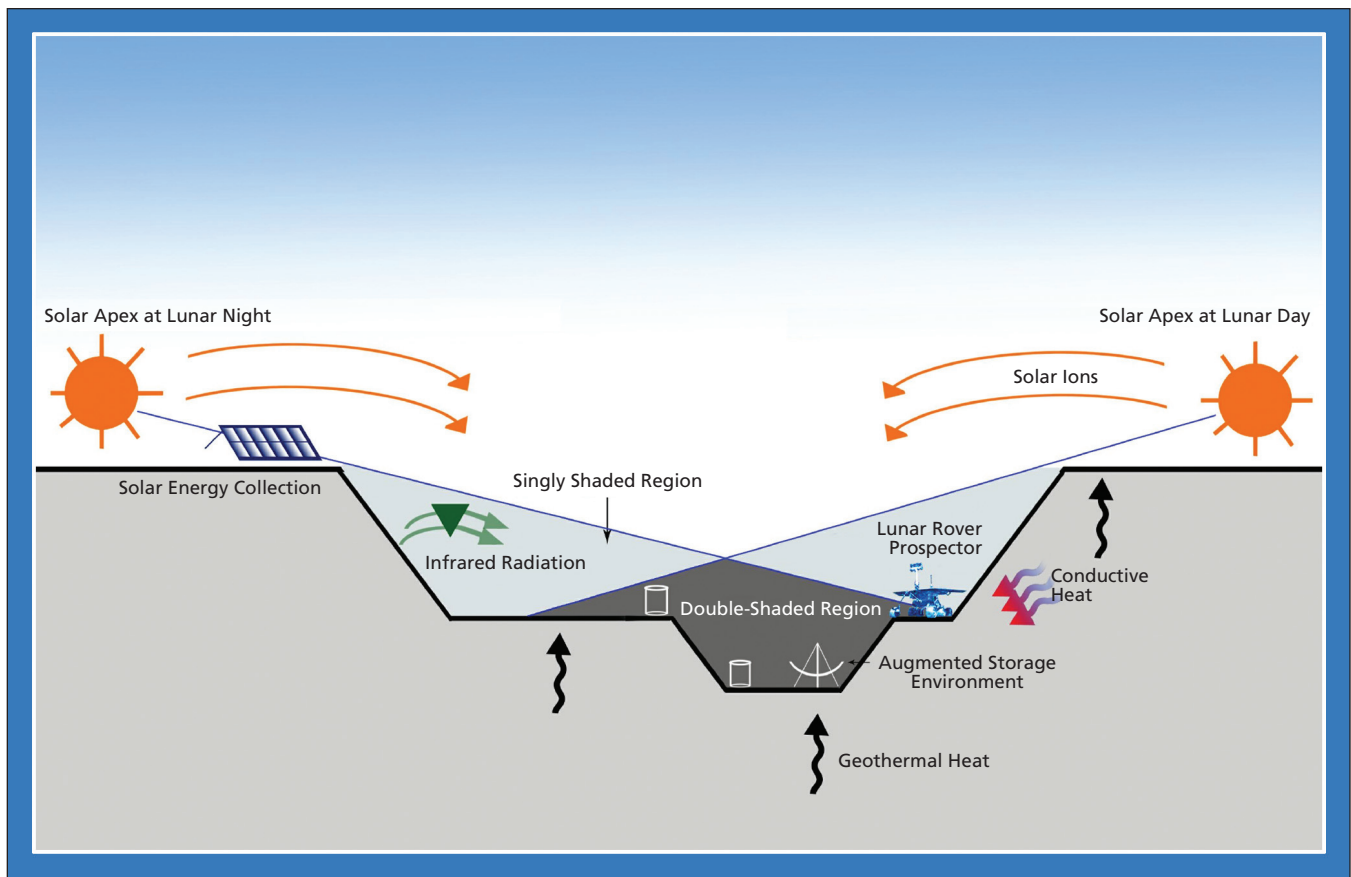
Stennis Space Center, Mississippi

In the polar regions of the Moon, some areas within craters are permanently shadowed from solar illumination and can drop to temperatures of 100 K or lower. These sites may serve as cold traps, capturing ice and other volatile compounds, possibly for eons. Interestingly, ice stored in these locations could potentially alter how lunar exploration is conducted. Within craters inside craters (double-shaded craters) that are shaded from thermal re-radiation and from solar illuminated regions, even colder regions should exist and, in many cases, temperatures in these regions never exceed 50 K. Working in these harsh environments with existing conventional systems, exploration or mining activities could be quite daunting and challenging. However, if the unique characteristics of these environments

were exploited, the power, weight, and total mass that is required to be carried from the Earth to the Moon for lunar exploration and research would be substantially reduced.

In theory, by minimizing the heat transfer between an object and the lunar surface, temperatures near absolute zero can be produced. In a single or double-shaded crater, if the object was isolated from the variety of thermal sources and was allowed to radiatively cool to space, the achievable temperature would be limited by the 3 K cosmic background and the anomalous solar wind that can strike the object being cooled. Our analysis shows that under many circumstances, with some simple thermal radiation shielding, it is possible to establish environments with temperatures of several de-

grees Kelvin. Electrostatic or other approaches for shielding from the solar wind and other high energy particles would enable the object to come into close thermal equilibrium with thermal cosmic background radiation. To minimize the heat transfer (conduction and radiation) between the ground and an object on the Moon (where the gravity is relatively small), a simple method to isolate even a relatively large object would be to use a low thermal insulating suspension structure that would hold both the thermal shield and the object above the thermal shield. The figure depicts a lunar polar region revealing a permanently shaded crater and a double-shaded crater. Within the double-shaded crater, a suspended thermal shield reflecting 50 K gray body radiation back towards the lunar



A Single- and a Double-Shaded Crater are shown on the lunar surface. Inside a double-shaded region within a single shaded crater, a thermal radiation shield reduces the heat transfer from the surface.

surface, is shown. Extremely low heat conduction between the object and the lunar surface could also be produced by using superconducting magnetic levitation, such as the Meissner Effect, to support the thermal shield and object. The thermal radiation shield should be shaped so that it blocks the lunar surface thermal radiation from all directions.

Advanced thermal management architecture based upon the augmentation of thermal conditions in these craters would be able to support a wide variety of cryogenically based applications. Lunar exploration and habitation capabilities would significantly benefit if permanently shaded craters, augmented with thermal shielding, were used to permit the operation of near-absolute-zero instruments, including an array of cryogenically based propulsion, energy, communication, sensing, and computing devices. For example, many gases used for life support or propulsion systems could be stored as solids, eliminating or minimizing the need for storage vessels. Storage of cryogens and other volatiles in solid form could substantially reduce the mass that would have to be launched from the Earth to the Moon. Addition-

ally, the ability to condense gases could serve as a means to purify air for breathing and other purposes.

Other uses for ultra-low temperature lunar craters (enhanced with artificial thermal radiation shielding) include the storage of biological samples, energy storage, advanced sensors, and even high-energy lasers for power transmission purposes. Since superconductors can theoretically store currents for billions of years, superconducting toroids serving as Superconducting Magnetic Energy Storage Systems could limitlessly store electrical energy from solar panels or other sources. Superconducting magnets could support a variety of applications, such as superconducting flywheel energy storage, drills, rail guns, and motors for vehicles. When cooled, semiconductor lasers can approach 100 percent wall-plug efficiency and could be used for transmitting power from one location to another. This technology could be used to beam power or information to land rovers and other mobile exploratory vehicles. Superconducting computers operating near terahertz clock speeds could potentially enable the development of consolidated, compact, high-end lunar-based computing devices.

Finally, these thermally cooled environments could also support the use of advanced magnetometers and infrared detector sensors. Additional augmentation to thermal environments with a hybrid passive and active cooling system could facilitate the operation of these sensors and other devices at temperatures as low as a fraction of a degree Kelvin, thereby enabling, for example, superfluid helium frictionless bearing devices for advanced gyroscopes. These colder temperatures could be used for many other technologies, like Transition Edge Sensors, that are used for radiation and infrared detection. In summary, permanently shaded polar craters in either their natural or augmented state could potentially reduce the required burden of carrying massive life-support components, mining tools, and research instrumentation from the Earth to the Moon.

This work was done by David Brannon of Stennis Space Center and Robert E. Ryan, Lauren W. Underwood, and Kristen Russell of Science Systems and Applications, Inc.

Inquiries concerning rights for the commercial use of this invention should be addressed to the Intellectual Property Manager at Stennis Space Center (228) 688-1929. Refer to SSC-00259-1.

Simultaneous Spectral Temporal Adaptive Raman Spectrometer — SSTARS

NASA's Jet Propulsion Laboratory, Pasadena, California

Raman spectroscopy is a prime candidate for the next generation of planetary instruments, as it addresses the primary goal of mineralogical analysis, which is structure and composition. However, large fluorescence return from many mineral samples under visible light excitation can render Raman spectra unattainable. Using the described approach, Raman and fluorescence, which occur on different time scales, can be simultaneously obtained from mineral samples using a compact instrument in a planetary environment. This new approach is taken based on the use of time-resolved spectroscopy for removing the fluorescence background from Raman spectra in the laboratory.

In the SSTARS instrument, a visible excitation source (a green, pulsed laser) is used to generate Raman and fluorescence signals in a mineral sample. A spectral notch filter eliminates the directly reflected beam. A grating then disperses the signal spectrally, and a streak camera provides temporal resolution. The output of the streak camera is imaged on the CCD (charge-coupled device), and the data are read out electronically. By adjusting the sweep speed of the streak camera, anywhere from picoseconds to milliseconds, it is possible to resolve Raman spectra from numerous fluorescence spectra in the same sample. The key features of SSTARS include a compact

streak tube capable of picosecond time resolution for collection of simultaneous spectral and temporal information, adaptive streak tube electronics that can rapidly change from one sweep rate to another over ranges of picoseconds to milliseconds, enabling collection of both Raman and fluorescence signatures versus time and wavelength, and Synchroscan integration that allows for a compact, low-power laser without compromising ultimate sensitivity.

This work was done by Jordana Blackberg of Caltech for NASA's Jet Propulsion Laboratory. Further information is contained in a TSP (see page 1), NPO-46752

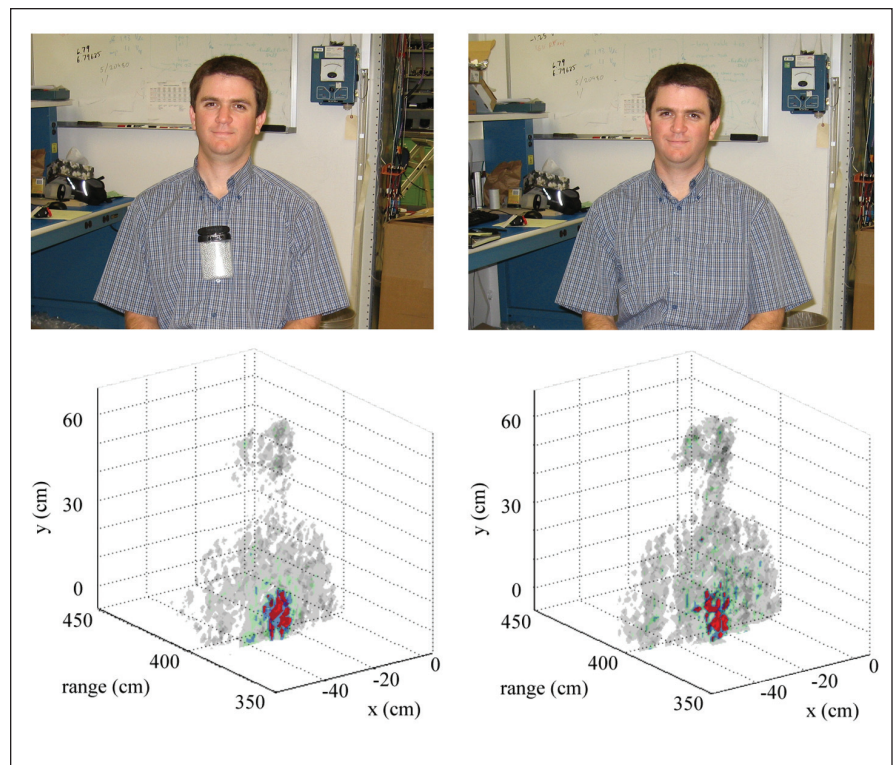
Improved Speed and Functionality of a 580-GHz Imaging Radar

This room-temperature, all-solid-state active submillimeter imager can be used to detect concealed weapons through clothing.

NASA's Jet Propulsion Laboratory, Pasadena, California

With this high-resolution imaging radar system, coherent illumination in the 576-to-589-GHz range and phase-sensitive detection are implemented in an all-solid-state design based on Schottky diode sensors and sources. By employing the frequency-modulated, continuous-wave (FMCW) radar technique, centimeter-scale range resolution has been achieved while using fractional bandwidths of less than 3 percent. The high operating frequencies also permit centimeter-scale cross-range resolution at several-meter standoff distances without large apertures. Scanning of a single-pixel transceiver enables targets to be rapidly mapped in three dimensions, so that the technology can be applied to the detection of concealed objects on persons.

The system evolved from a tunable, continuous-wave (CW) 600-GHz vector imager system. The radar's key components, custom-built for a different application at JPL, are the Schottky-diode multipliers generating transmit powers of 0.3 to 0.4 mW over 576 to 595 GHz and a balanced fundamental mixer exhibiting a double-sideband noise temperature of $\approx 4,000$ K over the same range. Also no-



Photographs (top) and 3D THz Radar Imager Reconstructions (bottom) of a person. On the left, the subject is wearing an exposed plastic container filled with ball bearings. On the right, the same container is concealed under his shirt.

table in the design is that residual phase-wander between the locked radio frequency (RF) and local oscillator (LO) K-band source synthesizers is canceled at an intermediate 450 MHz IF stage before final conversion to baseband through an IQ mixer.

To implement the FMCW chirp, a 2–4 GHz low-phase-noise commercial YIG synthesizer is used with a tuning bandwidth of 5 kHz, typically ramping over 350 MHz (subsequently multiplied by 36 to 12.6 GHz) in 50 ms. The chirp signal is up-converted onto the CW synthesizers' signals before multiplication. Deramping of the FMCW waveform occurs at the 600 GHz receiver mixer. While high multiplication factors should be generally avoided in FMCW radar systems to minimize the impact of phase noise in the transmitted signal, in this case, the short standoff ranges produce a phase noise floor that lies below the

thermal noise except for the brightest, mirrorlike specular targets.

The submillimeter power is transmitted first through a silicon wafer beam splitter and then a plano-convex Teflon lens with a diameter of 20 cm. This lens focuses the THz beam to a spot size of ≈ 2 cm at a standoff range of 4 m. To achieve scanned images, a flat mirror on a two-axis rotational stage deflects the beam in the desired direction.

This innovation is an improvement over an earlier submillimeter high-resolution radar. First, a faster frequency-sweeping method consisting of a wide-band YIG oscillator has been implemented. Second, the data acquisition and signal processing software has been updated in order to deal with the faster radar pulse repetition rate.

The improvements mean that the 580-GHz imaging radar can now acquire three-dimensional images of people in

about five minutes. It is also feasible to detect objects concealed by clothing. This capability is possible because of the improved speed and functionality of the imaging radar's hardware and software.

This work was done by Robert Dengler, Ken Cooper, Goutam Chattopadhyay, Peter Siegel, Erich Schlecht, Imran Mehdi, Anders Skalare, and John Gill of Caltech for NASA's Jet Propulsion Laboratory.

In accordance with Public Law 96-517, the contractor has elected to retain title to this invention. Inquiries concerning rights for its commercial use should be addressed to:

*Innovative Technology Assets Management
JPL*

Mail Stop 202-233

4800 Oak Grove Drive

Pasadena, CA 91109-8099

E-mail: iaoffice@jpl.nasa.gov

Refer to NPO-45156, volume and number of this NASA Tech Briefs issue, and the page number.

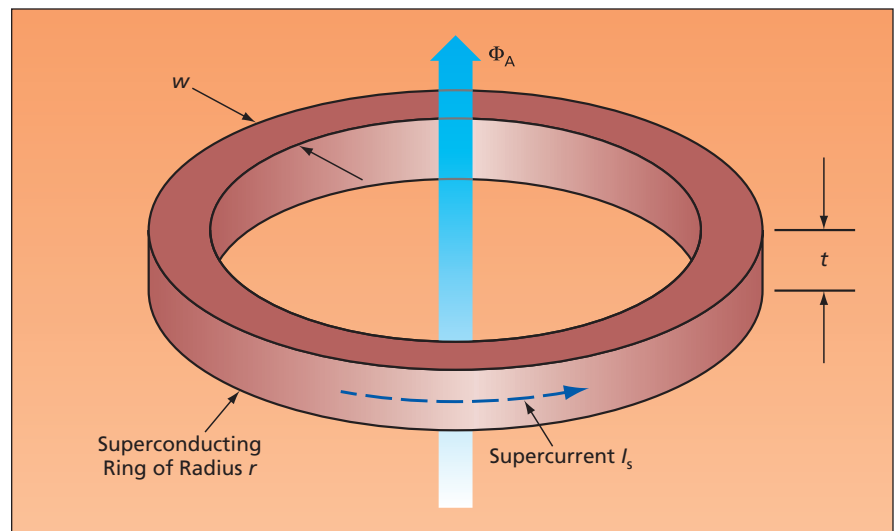
Bolometric Device Based on Fluxoid Quantization

This device offers extremely high sensitivity for radiometric applications.

NASA's Jet Propulsion Laboratory, Pasadena, California

The temperature dependence of fluxoid quantization in a superconducting loop. The sensitivity of the device is expected to surpass that of other superconducting-based bolometric devices, such as superconducting transition-edge sensors and superconducting nanowire devices. Just as important, the proposed device has advantages in sample fabrication. Two challenges of transition edge sensor fabrication are the reproducibility of the superconducting transition temperature, T_c , and the sharpness of the transition. In the proposed device, unlike in other devices, the sample would remain in the superconducting state at all times during operation. That is to say it would be maintained at an absolute temperature, T , below its superconducting T_c . Thus, the sharpness of the transition does not directly come into play. Also, the device can operate over a relatively wide temperature span of about $0.70 T_c$ to $0.95 T_c$. Therefore, reproducibility of T_c is not important from sample to sample. These two advantages eliminate major challenges in device fabrication.

The proposal is based on the theory of fluxoid quantization in a superconducting loop (see figure) with a track width (w) less than the temperature-depend-



A **Superconducting Ring** would support a temperature-dependent supercurrent I_s in the presence of an applied magnetic flux Φ_A .

ent characteristic depth of supercurrent penetration (λ) of the material. The theory has been shown to lead to the following equation:

$$I_s(T) = \frac{wt(n\Phi_0 - \Phi_A)}{2\pi r \mu_0 \lambda_0^2} [1 - (T/T_c)^4]$$

where I_s is the temperature-dependent supercurrent, t is the thickness of the su-

perconducting ring, Φ_0 is the magnetic-flux quantum, n is an integer denoting the number of fluxoid quanta, Φ_A is the magnetic flux applied to the ring, r is the radius of the ring, and λ_0 is the characteristic depth of penetration of supercurrent at absolute zero temperature.

The applied magnetic flux (Φ_A) would serve as a bias that could be adjusted to select the mode of operation.

This flux could be generated by any convenient means — such as those used to flux bias DC-SQUIDS. To obtain one of two distinct modes of operation, one would adjust Φ_A to obtain $n\Phi_0 - \Phi_A \approx \Phi_0/2$, placing the device in the middle of the n -fluxoid quanta branch. This mode would be a radiometric one, in which the device would function similarly to a superconducting-transition-edge sensor (TES) bolometer. Assuming the proposed device would be mounted on a low-thermal-conductance membrane similar to that used for TES bolometers, it has been estimated that

the responsivity would be an order of magnitude greater than that of a typical TES bolometer.

To obtain the other distinct mode of operation, one would adjust Φ_A to place the device extremely close to the transition between the n - and $(n - 1)$ -fluxoid quanta branches. In this mode, the device would function as a threshold-type sensor having potential utility in applications that involve photon counting and other counting-type detections.

This work was done by Joseph A. Bonetti, Matthew E. Kenyon, Henry G. Leduc, and Peter K. Day of Caltech for NASA's Jet Propul-

sion Laboratory. Further information is contained in a TSP (see page 1).

In accordance with Public Law 96-517, the contractor has elected to retain title to this invention. Inquiries concerning rights for its commercial use should be addressed to:

*Innovative Technology Assets Management
JPL*

Mail Stop 202-233

4800 Oak Grove Drive

Pasadena, CA 91109-8099

E-mail: iaoffice@jpl.nasa.gov

Refer to NPO-45655, volume and number of this NASA Tech Briefs issue, and the page number.



➤ Algorithms for Learning Preferences for Sets of Objects

The user gives examples of preferred sets; the algorithms do the rest.

NASA's Jet Propulsion Laboratory, Pasadena, California

A method is being developed that provides for an artificial-intelligence system to learn a user's preferences for sets of objects and to thereafter automatically select subsets of objects according to those preferences. The method was originally intended to enable automated selection, from among large sets of images acquired by instruments aboard spacecraft, of image subsets considered to be scientifically valuable enough to justify use of limited communication resources for transmission to Earth. The method is also applicable to other sets of objects: examples of sets of objects considered in the development of the method include food menus, radio-station music playlists, and assortments of colored blocks for creating mosaics.

The method does not require the user to perform the often-difficult task of quantitatively specifying preferences; instead, the user provides examples of preferred sets of objects. This method goes beyond related prior artificial-intelligence methods for learning which individual items are preferred by the user:

this method supports a concept of set-based preferences, which include not only preferences for individual items but also preferences regarding types and degrees of diversity of items in a set. Consideration of diversity in this method involves recognition that members of a set may interact with each other in the sense that when considered together, they may be regarded as being complementary, redundant, or incompatible to various degrees. The effects of such interactions are loosely summarized in the term "portfolio effect."

The learning method relies on a preference representation language, denoted DD-PREF, to express set-based preferences. In DD-PREF, a preference is represented by a tuple that includes quality ("depth") functions to estimate how desired a specific value is, weights for each feature preference, the desired diversity of feature values, and the relative importance of diversity versus depth. The system applies statistical concepts to estimate quantitative measures of the user's preferences from training examples (preferred subsets) specified by the user.

Once preferences have been learned, the system uses those preferences to select preferred subsets from new sets.

The method was found to be viable when tested in computational experiments on menus, music playlists, and rover images. Contemplated future development efforts include further tests on more diverse sets and development of a submethod for (a) estimating the parameter that represents the relative importance of diversity versus depth, and (b) incorporating background knowledge about the nature of quality functions, which are special functions that specify depth preferences for features.

This work was done by Kiri L. Wagstaff of Caltech and Marie desJardins and Eric Eaton of the University of Maryland, Baltimore County, for NASA's Jet Propulsion Laboratory. Further information is contained in a TSP (see page 1).

The software used in this innovation is available for commercial licensing. Please contact Daniel Broderick of the California Institute of Technology at danielb@caltech.edu. Refer to NPO-43828.

➤ Model for Simulating a Spiral Software-Development Process

A prior model for simulating a waterfall process has been extended.

John F. Kennedy Space Center, Florida

A discrete-event simulation model, and a computer program that implements the model, have been developed as means of analyzing a spiral software-development process. This model can be tailored to specific development environments for use by software project managers in making quantitative cases for deciding among different software-development processes, courses of action, and cost estimates.

A spiral process can be contrasted with a waterfall process, which is a traditional process that consists of a sequence of activities that include analysis of requirements, design, coding, testing, and support. A spiral process is an

iterative process that can be regarded as a repeating modified waterfall process. Each iteration includes assessment of risk, analysis of requirements, design, coding, testing, delivery, and evaluation. A key difference between a spiral and a waterfall process is that a spiral process can accommodate changes in requirements at each iteration, whereas in a waterfall process, requirements are considered to be fixed from the beginning and, therefore, a waterfall process is not flexible enough for some projects, especially those in which requirements are not known at the beginning or may change during

development. For a given project, a spiral process may cost more and take more time than does a waterfall process, but may better satisfy a customer's expectations and needs.

Models for simulating various waterfall processes have been developed previously, but until now, there have been no models for simulating spiral processes. The present spiral-process-simulating model and the software that implements it were developed by extending a discrete-event simulation process model of the IEEE 12207 Software Development Process, which was built using commercially available software known as the

Process Analysis Tradeoff Tool (PATT). Typical inputs to PATT models include industry-average values of product size (expressed as number of lines of code), productivity (number of lines of code per hour), and number of defects per source line of code. The user provides the number of resources, the overall percent of effort that should be allocated to each process step, and the number of desired staff members for each step. The output of PATT includes the size of the product, a measure of effort, a measure of rework effort, the duration of the entire process,

and the numbers of injected, detected, and corrected defects as well as a number of other interesting features.

In the development of the present model, steps were added to the IEEE 12207 waterfall process, and this model and its implementing software were made to run repeatedly through the sequence of steps, each repetition representing an iteration in a spiral process. Because the IEEE 12207 model is founded on a waterfall paradigm, it enables direct comparison of spiral and waterfall processes. The model can be

used throughout a software-development project to analyze the project as more information becomes available. For instance, data from early iterations can be used as inputs to the model, and the model can be used to estimate the time and cost of carrying the project to completion.

This work was done by Carolyn Mizell of Kennedy Space Center, Charles Curley of ASRC Aerospace Corp., and Umanath Nayak of Portland State University. Further information is contained in a TSP (see page 1). KSC-13094

➤ Algorithm That Synthesizes Other Algorithms for Hashing

A synthesized algorithm is guaranteed to be executable in constant time.

NASA's Jet Propulsion Laboratory, Pasadena, California

An algorithm that includes a collection of several subalgorithms has been devised as a means of synthesizing still other algorithms (which could include computer code) that utilize hashing to determine whether an element (typically, a number or other datum) is a member of a set (typically, a list of numbers). Each subalgorithm synthesizes an algorithm (e.g., a block of code) that maps a static set of key hashes to a somewhat linear monotonically increasing sequence of integers. The goal in formulating this mapping is to cause the length of the sequence thus generated to be as close as practicable to the original length of the set and thus to minimize gaps between the elements.

The advantage of the approach embodied in this algorithm is that it completely avoids the traditional approach

of hash-key look-ups that involve either secondary hash generation and look-up or further searching of a hash table for a desired key in the event of collisions.

This algorithm guarantees that it will never be necessary to perform a search or to generate a secondary key in order to determine whether an element is a member of a set. This algorithm further guarantees that any algorithm that it synthesizes can be executed in constant time. To enforce these guarantees, the subalgorithms are formulated to employ a set of techniques, each of which works very effectively covering a certain class of hash-key values. These subalgorithms are of two types, summarized as follows:

- Given a list of numbers, try to find one or more solutions in which, if each number is shifted to the right by a con-

stant number of bits and then masked with a rotating mask that isolates a set of bits, a unique number is thereby generated. In a variant of the foregoing procedure, omit the masking. Try various combinations of shifting, masking, and/or offsets until the solutions are found. From the set of solutions, select the one that provides the greatest compression for the representation and is executable in the minimum amount of time.

- Given a list of numbers, try to find one or more solutions in which, if each number is compressed by use of the modulo function by some value, then a unique value is generated.

This work was done by Mark James for Caltech for NASA's Jet Propulsion Laboratory. Further information is contained in a TSP (see page 1). NPO-45175

➤ Algorithms for High-Speed Noninvasive Eye-Tracking System

One of the algorithms enables tracking at a frame rate of several kilohertz.

NASA's Jet Propulsion Laboratory, Pasadena, California

Two image-data-processing algorithms are essential to the successful operation of a system of electronic hardware and software that noninvasively tracks the direction of a person's gaze in real time. The system was described in "High-Speed Noninvasive Eye-Tracking System" (NPO-30700) *NASA Tech Briefs*, Vol. 31, No. 8 (August 2007), page 51.

To recapitulate from the cited article: Like prior commercial noninvasive eye-

tracking systems, this system is based on (1) illumination of an eye by a low-power infrared light-emitting diode (LED); (2) acquisition of video images of the pupil, iris, and cornea in the reflected infrared light; (3) digitization of the images; and (4) processing the digital image data to determine the direction of gaze from the centroids of the pupil and cornea in the images. Most of the prior commercial noninvasive eye-

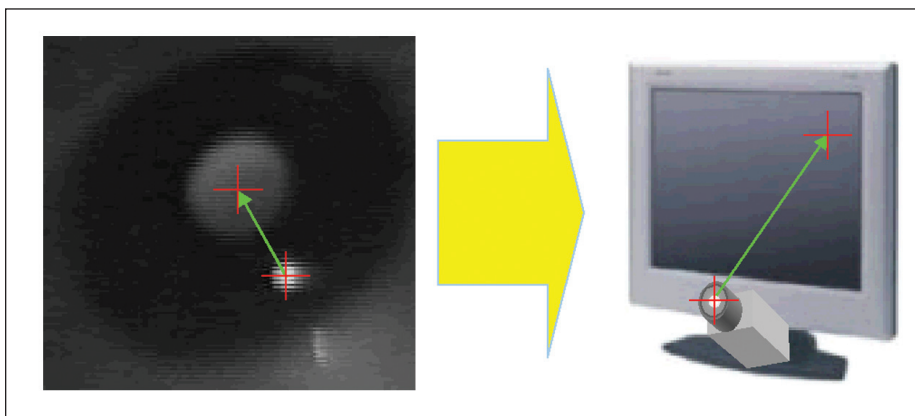
tracking systems rely on standard video cameras, which operate at frame rates of about 30 Hz. Such systems are limited to slow, full-frame operation.

The video camera in the present system includes a charge-coupled-device (CCD) image detector plus electronic circuitry capable of implementing an advanced control scheme that effects readout from a small region of interest (ROI), or subwindow, of the full image. Inas-

much as the image features of interest (the cornea and pupil) typically occupy a small part of the camera frame, this ROI capability can be exploited to determine the direction of gaze at a high frame rate by reading out from the ROI that contains the cornea and pupil (but not from the rest of the image) repeatedly.

One of the present algorithms exploits the ROI capability. The algorithm takes horizontal row slices and takes advantage of the symmetry of the pupil and cornea circles and of the gray-scale contrasts of the pupil and cornea with respect to other parts of the eye. The algorithm determines which horizontal image slices contain the pupil and cornea, and, on each valid slice, the end coordinates of the pupil and cornea. Information from multiple slices is then combined to robustly locate the centroids of the pupil and cornea images.

The other of the two present algorithms is a modified version of an older algorithm for estimating the direction of gaze from the centroids of the pupil and cornea. The modification lies in the use of the coordinates of the centroids, rather than differences between the coordinates of the centroids, in a gaze-



The **Vector Between the Centroids** of pupil and corneal reflections is computed and then used to compute the direction of gaze and the gaze point.

mapping equation. The equation locates a gaze point, defined as the intersection of the gaze axis with a surface of interest, which is typically a computer display screen (see figure). The expected advantage of the modification is to make the gaze computation less dependent on some simplifying assumptions that are sometimes not accurate.

This work was done by Ashit Talukder, John-Michael Morookian, and James Lambert of Caltech for NASA's Jet Propulsion Laboratory. Further information is contained in a TSP (see page 1).

In accordance with Public Law 96-517, the contractor has elected to retain title to this invention. Inquiries concerning rights for its commercial use should be addressed to:

*Innovative Technology Assets Management
JPL*

Mail Stop 202-233

4800 Oak Grove Drive

Pasadena, CA 91109-8099

E-mail: iaoffice@jpl.nasa.gov

Refer to NPO-30699, volume and number of this NASA Tech Briefs issue, and the page number.

➤ Adapting ASPEN for Orbital Express

Declarative modeling brings efficiency to encoded procedures and allows for guarantees on resource usage and time usage.

NASA's Jet Propulsion Laboratory, Pasadena, California

By studying the Orbital Express mission, modeling the spacecraft and scenarios, and testing the system, a technique has been developed that uses recursive decomposition to represent procedural actions declaratively, schema-level uncertainty reasoning to make uncertainty reasoning tractable, and lightweight, natural language processing to automatically parse procedures to produce declarative models.

Schema-level uncertainty reasoning has, at its core, the basic assumption that certain variables are uncertain, but not independent. Once any are known, then the others become known. This is important where a variable is uncertain for an action and many actions of the same type exist in the plan. For example, if the number of retries to purge pump lines was unknown (but bounded), and each attempt required a sub-plan, then,

once the correct number of attempts required for a purge was known, it would likely be the same for all subsequent purges. This greatly reduces the space of plans that needs to be searched to ensure that all executions are feasible.

To accommodate changing scenario procedures, each is ingested into a tabular format in temporal order, and a simple natural-language parser is used to read each step and to derive the impact of that step on memory, power, and communications. Then an ASPEN (Activity Scheduling and Planning Environment) model is produced based on this analysis. The model is tested and further changed by hand, if necessary, to reflect the actual procedure. This results in a great savings of time used for modeling procedures.

Many processes that need to be modeled in ASPEN (a declarative system)

are, in fact, procedural. ASPEN includes the ability to model activities in a hierarchical fashion, but this representation breaks down if there is a practically unbounded number of sub-activities and decomposition topologies. However, if recursive decomposition is allowed, HTN-like encodings are enabled to represent most procedural phenomena.

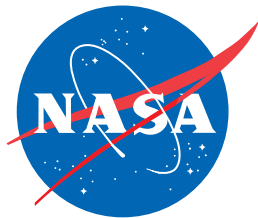
For example, if a switch requires a variable (but known at the time of the attempt) number of attempts to switch on, one can recurse on the number of remaining switch attempts and decompose into either the same switching activity with one less required attempt, or not decompose at all (or decompose into a dummy task), resulting in the end of the decomposition. In fact, any bounded procedural behavior can be modeled using recursive decompositions assuming that the variables impinging the dis-

conjunctive decomposition decision are computable at the time that the decision is made. This enables one to represent tasks that are controlled outside of the scheduler, but that the scheduler must accommodate, without requiring one to

give a declarative model of the procedural behavior.

This work was done by Caroline Chouinard, Daniel Tran, Grailing Jones, Van Dang, and Russell Knight of Caltech for NASA's Jet Propulsion Laboratory.

The software used in this innovation is available for commercial licensing. Please contact Daniel Broderick of the California Institute of Technology at danielb@caltech.edu. Refer to NPO-45262.



National Aeronautics and
Space Administration